

Dancing in the Dark: Satellites of dwarf galaxies as probes of the first star formation

FERAH MUNSHI,^{1,2,3} ALYSON M. BROOKS,³ CHARLOTTE CHRISTENSEN,⁴ ELAAD APPLEBAUM,³
 KELLY HOLLEY-BOCKELMANN,² THOMAS R. QUINN,⁵ AND JAMES WADSLEY⁶

¹*Department of Physics & Astronomy, University of Oklahoma
 440 W. Brooks St., Norman, OK 73019*

²*Department of Physics & Astronomy, Vanderbilt University
 6301 Stevenson Center, Vanderbilt University, Nashville, TN 37235*

³*Department of Physics & Astronomy, Rutgers, The State University of New Jersey
 136 Frelinghuysen Rd, Piscataway, NJ 08854*

⁴*Department of Physics & Astronomy, Grinnell University
 Grinnell, IA 50112*

⁵*Department of Astronomy, University of Washington
 3910 15th Ave., Seattle, WA 98195*

⁶*Department of Physics & Astronomy, McMaster University
 Hamilton, Ontario L8S 4K1*

Abstract

The existence of ultra-faint dwarf (UFD) galaxies highlights the need to push our theoretical understanding of galaxies to extremely low mass. Using two identical high-resolution, fully cosmological simulations of dwarf galaxies, we examine the formation of dwarf galaxies and their UFD satellites. The simulations have identical initial conditions, and vary only in how they form stars: one uses a temperature-density threshold for star formation in combination with metal line cooling, while the other replaces the temperature-density threshold with an H₂-based sub-grid star formation model. We find that the total number of dwarf galaxies that forms is different by a factor of 2 between the two runs, but most of these are satellites, leading to a factor of 5 difference in the number of luminous UFD companions around more massive, isolated dwarfs. The metal-cooling (MC) run yields 10 resolved luminous satellites, a 47% chance of finding a satellite around a $M_{halo} \sim 10^{10} M_{\odot}$ host. The H₂ run, on the other hand, produces only two luminous satellites, and predicts only a 16% chance of finding a luminous satellite around the same sized host. Metallicity is the primary physical parameter that creates this difference. As metallicity decreases, the formation of H₂ is slowed and relegated to higher-density material. Thus, our H₂ run is unable to form many (and often, any) stars before reionization removes gas. These results emphasize that predictions for UFD properties made using hydrodynamic simulations, in particular regarding the frequency of satellites around dwarf galaxies, the slope of the stellar mass function at low masses, as well as the properties of ultra-faint galaxies occupying the smallest halos, are extremely sensitive to the subgrid physics of star formation contained within the simulation. However, upcoming discoveries of ultra-faint dwarfs both in the Milky Way halo and in the Local Group will provide invaluable constraining power on the physics of the first star formation.

1. INTRODUCTION

The favored Λ Cold Dark Matter (Λ CDM) cosmological model predicts that structure formation is self-similar. All dark matter halos should contain an abundance of dark matter substructure, from the largest galaxy cluster halos, to the smallest halos containing observed dwarf galaxies, and beyond. The scale-free nature of the subhalo mass function in Λ CDM suggests that groups of subhalos should be common (Li & Helmi 2008; D’Onghia & Lake 2008; Sales et al. 2011; Nichols et al. 2011). Because low-mass halos form earlier, are denser,

and fall into smaller hosts before larger ones, it is likely that satellites of satellites or of low mass isolated halos have survived longer than their counterparts that fell directly into the Milky Way (Diemand et al. 2005). This suggests that one way to search for ultra-faint galaxies might be to search for satellites of known dwarf galaxies (Rashkov et al. 2012; Sales et al. 2013; Wheeler et al. 2015; Carlin et al. 2016; Dooley et al. 2017b; Patel et al. 2018).

Recently, the *Dark Energy Survey* (DES), has nearly doubled the number of known UFDs in the Milky Way (Bechtol et al. 2015; Drlica-Wagner et al. 2015;

Kim & Jerjen 2015; Kim et al. 2015; Koposov et al. 2015; Luque et al. 2017). Many of the DES dwarfs are thought to potentially be satellites of the Magellanic Cloud system (Deason et al. 2015; Yozin & Bekki 2015; Jethwa et al. 2016; Sales et al. 2017; Kallivayalil et al. 2018; Li et al. 2018). These UFD detections, combined with surveys like SMASH (Martin et al. 2015), PanSTARRS (Laevens et al. 2015), ATLAS (Torrealba et al. 2016), *Hyper Suprime-Cam Subaru Strategic Program* (HSC-SSP, Homma et al. 2018), and MagLiteS (Drlica-Wagner et al. 2016), have opened up a new galaxy discovery space, providing an exciting glimpse into the frontier of galaxy formation in the smallest halos.

Combined with classical dwarfs, observations are beginning to probe the full range of dwarf galaxy masses, a key step in understanding the complex interplay between feedback, reionization and halo mass on star formation history and enrichment.

Dooley et al. (2017b) used a range of Stellar Mass – Halo Mass (SMHM) relations derived from abundance matching results combined with a model for reionization to constrain the expected number of UFD satellite companions of Local Group dwarf galaxies. When applied directly to the Magellanic Clouds (Dooley et al. 2017a), they find that $\sim 50\%$ of satellites within 50 kpc of the LMC have been accreted with the Magellanic Cloud system. Moreover, they show that within 300 kpc of the MW, 10–15% of all satellites smaller than the SMC were accreted with the LMC, and 5–10% with the SMC. As such, it becomes clear that isolated dwarfs in the Local Group are extremely interesting targets in the hunt for ever-fainter dwarfs.

However, how many of these subhalos of subhalos should be populated with stars is still an open question. In fact, our current simple models for how dwarf galaxies populate halos may be at odds with the observations (Dooley et al. 2017a). Λ CDM galaxy simulations show that the subhalo mass function rises steadily to masses below the molecular cooling limit ($M_{halo} \gtrsim 10^6 M_{\odot}$ Haiman et al. 1996; Abel et al. 2002; Bromm et al. 2002; Visbal et al. 2015), but populating all of the simulated halos with galaxies leads to abundance matching problems (Madau et al. 2008; Bovill & Ricotti 2011; Dooley et al. 2017a). Gas is inefficient at cooling in halos with virial temperatures less than 10^4 K ($M_{halo} \sim 10^7 M_{\odot}$; e.g., Haiman et al. 1997), but there may be other processes at play that create a low-mass cutoff in galaxy formation.

The heating of accreted gas or the prevention of gas accretion by the ionizing UV background at the epoch of reionization can stop or even prevent star

formation in the smallest dark matter halos, suggesting a threshold in halo mass below which all halos remain dark (Gnedin 2000; Somerville 2002; Benson et al. 2002; Kravtsov et al. 2004; Simon & Geha 2007; Okamoto et al. 2008; Kuhlen et al. 2012; O’Shea et al. 2015). Many have shown that this photoheating prevents gas from condensing in halos with masses $\sim 10^{8-9} M_{\odot}$ (Okamoto & Frenk 2009; Nickerson et al. 2011; Sawala et al. 2012; Shen et al. 2014; Wheeler et al. 2015; Visbal et al. 2017). It is possible, however, that halos at lower masses are able to form stars before reionization, making it unclear what the lowest halo mass is that should contain stars (e.g., Bullock et al. 2000; Li et al. 2014; Oñorbe et al. 2015; Bland-Hawthorn et al. 2015; Ocvirk et al. 2016; Jeon et al. 2017; Corlies et al. 2018).

In essence, the specific timing of the onset and end of reionization, the spectrum of the background radiation, the ability of gas to temporarily shield itself from these high energy photons, and the mass resolution and simulation star formation and feedback prescriptions, can have a large effect on the number and minimum halo mass of galaxies in any simulation (Efstathiou 1992; Dijkstra et al. 2004; Hoeft et al. 2006; Bromm & Yoshida 2011; Visbal et al. 2014; Pawlik et al. 2015; Oñorbe et al. 2017; Kuhlen et al. 2012).

Ideally, inferences from observations can be used to constrain the lowest mass halos that can form galaxies. Jethwa et al. (2018) found that halos at least down to $2.4 \times 10^8 M_{\odot}$ must be able to form galaxies in order to be consistent with the abundance of dwarfs found in the Local Group.¹ In a similar approach, but using HI gas content instead of stellar content, Tollerud & Peek (2018) put a limit on the lowest mass halo able to retain gas during reionization at $3 \times 10^8 M_{\odot}$. These results are at odds with simulations in which stars do not form until halos reach $10^9 M_{\odot}$ (e.g., Shen et al. 2014; Sawala et al. 2016).

As cosmological simulations of Milky Way-mass galaxies continue to achieve ever-higher resolution, they are on the verge of being able to resolve galaxies in the UFD range. With their ability to capture a broad range of processes including reionization, feedback from stars, supernovae, and AGN, as well as the details of mergers and subsequent tidal evolution, these simulations may be able to shed light on the observed UFD distribu-

¹ This is the peak halo mass over the age of the Universe, and translates into a $z = 0$ halo mass of $\sim 10^8 M_{\odot}$ for satellites after tidal stripping, consistent with inferences from observations of the Milky Way satellites, (e.g., Errani et al. 2018).

tion and the expected number of satellites around dwarf galaxies. In this paper we investigate one factor that is likely to lead to widely varying predictions: the fact that star formation prescriptions vary across simulations.

One of the key differences in star formation recipes between different galaxy simulations is the threshold mass density at which star formation is allowed to occur. By definition, lower resolution simulations do not have the ability to resolve high density gas peaks. Thus, the density threshold must vary with resolution of the simulation. Star formation density thresholds vary from $\sim 1 m_H \text{ cm}^{-3}$, where m_H is the mass of a hydrogen atom, in lower resolution simulations (e.g., APOSTLE, Fattahi et al. 2016) to $10 m_H \text{ cm}^{-3}$ (e.g., NIHAO Wang et al. 2015) to $> 100 m_H \text{ cm}^{-3}$ (e.g., Governato et al. 2010; Dobbs et al. 2011; Hopkins et al. 2014, 2018; Read et al. 2016). A maximum temperature threshold for star formation is also usually applied. Many simulations adopt a temperature cap of $\sim 10^4 \text{ K}$ because this is the peak of the cooling curve and gas is expected to rapidly cool to lower temperatures (e.g., see Saitoh et al. 2008).

Beyond this temperature-density model, some simulators also track the presence of molecular hydrogen, H_2 , requiring that it be present in order to form stars. The H_2 -based star formation models broadly break down into two categories, equilibrium (Krumholz et al. 2008, 2009; Kuhlen et al. 2012; Hopkins et al. 2014, 2018) or non-equilibrium (Robertson & Kravtsov 2008; Gnedin et al. 2009a; Gnedin & Kravtsov 2010, 2011; Christensen et al. 2012). Both models, by requiring the presence of H_2 , ensure that stars form from high density gas: generally star formation occurs in gas with $n > 100 m_H \text{ cm}^{-3}$ but it can be as high as $n > 1000 m_H \text{ cm}^{-3}$ depending on metallicity and resolution. The temperature cap for star formation is also usually lowered in these models as additional cooling processes are captured. However, the equilibrium models do not explicitly track the formation and destruction of H_2 , but rather assume a two-phase interstellar medium in which formation and destruction are balanced, thereby eliminating any sort of dependency on the timescale of H_2 formation. In the non-equilibrium model, the formation and destruction of H_2 are followed. We show in this paper that the delay in H_2 formation times at low metallicities in non-equilibrium models leads to a quantitative difference in the ability of UFD galaxies to form stars compared to temperature-density threshold models.

A number of authors have demonstrated that the density threshold for star formation has no impact on the star formation rate (SFR) of a simulated galaxy because

galaxies “self-regulate,” i.e., a change in the star formation density threshold is counter-balanced by subsequent feedback (Saitoh et al. 2008; Hopkins et al. 2011, 2013; Christensen et al. 2014b; Benincasa et al. 2016; Hopkins et al. 2018; Pallottini et al. 2017). These previous studies found that self-regulation can occur as long as the resolution is high enough to capture the average densities in giant molecular clouds (GMCs), and therefore that the simulation is high enough resolution to have star formation limited to the scales of GMCs (Agertz & Kravtsov 2016; Semenov et al. 2016). An exception is Kuhlen et al. (2012), which showed that an H_2 -based star formation prescription could dramatically suppress star formation in low mass halos where metallicities are low (and thus H_2 is unable to form). However, this is overcome in H_2 formation models if dense gas is able to shield and form H_2 despite low metallicities when sufficiently high resolutions are achieved (e.g., Hopkins et al. 2013). Another exception is Semenov et al. (2018), who show that self-regulation is limited to the regime of strong feedback, which regulates the gas supply available to turn into stars.

The two star formation prescriptions that we explore in this paper were also adopted in Christensen et al. (2014b, “Metals” and “ H_2 ” in that work), where it was shown that both models produce dwarf galaxies with nearly identical structural parameters (rotation curves, dark matter density profiles, baryonic angular momentum distributions) for galaxies with $\sim 10^8 M_\odot$ in stellar mass. Only the mass in galactic winds varied, but by less than a factor of two.

We show in this work that, although these star formation prescriptions lead to similar galaxies in the classical dwarf galaxy mass range, differences arise on the scale of UFDs.

This has important ramifications, e.g., for the slope and scatter at the faint-end of the SMHM relation and the slope of the stellar mass function in the ultra-faint regime (Lin & Ishak 2016; Munshi et al. 2017). In this paper we also emphasize the impact on the expected number of UFD satellites in dwarf galaxies.

The paper is organized as follows: we describe our simulations in Section 2. In Section 3 we quantify the occupation fraction of dark matter halos as a function of declining halo mass, and show that at the lowest halo masses there is a drastic difference in the number of luminous dwarf galaxy satellites in simulations with different star formation prescriptions. We find that the inability of low mass halos to form H_2 in the reionization epoch suppresses star formation relative to the same halos run with a temperature-density threshold star formation model. We discuss some implications and open

questions based on our results in Section 4. We summarize in Section 6.

2. THE SIMULATIONS

The simulations used in this work are run with the N-Body + Smoothed Particle Hydrodynamics (SPH) code CHANGA (Menon et al. 2015) in a fully cosmological Λ CDM context using WMAP Year 3 cosmology: $\Omega_0 = 0.26$, $\Lambda = 0.74$, $h = 0.73$, $\sigma_8 = 0.77$, $n = 0.96$. CHANGA utilizes the CHARM++ run-time system for dynamic load balancing and computation/communication overlap in order to effectively scale up the number of cores. This improved scaling has allowed for the simulation of large, high-resolution volumes (e.g., Tremmel et al. 2017; Anderson et al. 2017) that were previously unattainable with CHANGA’s predecessor code, GASOLINE, and we use this scaling here to simulate a volume of dwarf galaxies. CHANGA adopts all the same physics modules (described below) as GASOLINE, but has an improved SPH implementation that uses the geometric mean density to more realistically model the gas physics at the hot-cold interface (Wadsley et al. 2017). The developers of CHANGA are part of the AGORA collaboration, which aims to compare the implementation of hydrodynamics across cosmological codes (Kim et al. 2014, 2016).

Our galaxy sample is drawn from a uniform dark matter-only simulation of a 25 Mpc per side cube. From this volume, we select a field-like region representing a cosmological “sheet” roughly 3 Mpc in diameter, containing almost 7000 isolated dark matter halos from $2 \times 10^{10} M_\odot$ in halo mass down to our resolution limit of $4.3 \times 10^5 M_\odot$ (64 particles). We then re-simulate this field at extremely high resolution using the “zoomed-in” volume renormalization technique (Katz & White 1993; Pontzen et al. 2008). The zoom-in technique allows for high resolution in the region of interest, while accurately capturing the tidal torques from large scale structure that deliver angular momentum to galaxy halos (Barnes & Efstathiou 1987). These zoom-in simulations have a hydrodynamical smoothing length as small as 6 pc, a gravitational force softening of 60 pc, and an equivalent resolution to a 4096^3 particle grid. Dark matter particles have a mass of $6650 M_\odot$, while gas particles begin with a mass of $1410 M_\odot$, and star particles are born with 30% of their parent gas particle mass. The dark matter-only version of this volume was run in both a CDM and self-interacting dark matter (SIDM) model in Fry et al. (2015). Following the convention in that paper, we adopt the nickname “The 40 Thieves.”

METAL COOLING (MC):The “Metal Cooling (MC)” version of the 40 Thieves includes cooling of the gas

via primordial and metal-line cooling as well as diffusion of metals (Shen et al. 2010) in the ISM, and non-equilibrium abundances of H and He. Additionally, we adopt a simple model for self-shielding of the HI gas following Pontzen et al. (2008). Stars form based on a gas density threshold comparable to the mean density of molecular clouds and is similar to that described in Governato et al. (2010). Simply, star formation occurs stochastically when gas particles become cold ($T < 10^4$ K) and when gas reaches a density threshold of $100 m_H \text{ cm}^{-3}$. The probability, p , of spawning a star particle is a function of the local dynamical time t_{form} :

$$p = \frac{m_{\text{gas}}}{m_{\text{star}}} \left(1 - e^{-c^* \Delta t / t_{\text{form}}} \right) \quad (1)$$

where m_{gas} is the mass of the gas particle and m_{star} is the initial mass of the potential star particle. A star formation efficiency parameter, $c^* = 0.1$, gives the correct normalization of the Kennicutt-Schmidt relation (Christensen et al. 2014b).

MOLECULAR HYDROGEN (H_2):The “Molecular Hydrogen (H_2)” version of the 40 Thieves includes the aforementioned metal line cooling and metal diffusion (Shen et al. 2010) with the addition of non-equilibrium H_2 abundances and H_2 -based star formation. Our H_2 abundance calculation includes a gas-phase and dust-dependent description of H_2 creation, destruction by Lyman-Werner radiation, and shielding of HI and H_2 based on particle metallicity (Gnedin et al. 2009b; Christensen et al. 2012, hereafter CH12). As in CH12, the SFR in this simulation is set by the local gas density and the H_2 fraction. The star formation probability is again given by equation 1, but c^* is modified such that $c^* = c_0^* X_{H_2}$, where $c_0^* = 0.1$ and X_{H_2} is the fraction of baryons in H_2 . We restrict star formation to occur in gas particles with $T < 10^3$ K. With the inclusion of the H_2 fraction term, gas in low-metallicity dwarfs tends to reach even higher densities (required for the gas to shield and form H_2) than the MC model before it can form stars (Christensen et al. 2014b).

We apply a uniform, time-dependent UV field from Haardt & Madau (2012) to model photoionization and photoheating for both runs. Both simulations adopt the “blastwave” supernova feedback approach (Stinson et al. 2006), in which mass, thermal energy, and metals are deposited into nearby gas when massive stars evolve into supernovae. The thermal energy deposited amongst those nearby gas neighbors is 10^{51} ergs per supernova event. Following Stinson et al. (2010), we quantize the feedback so that supernovae only occur when whole stars have gone supernova, as opposed to slowly releasing fractions of supernova energy at every

time step. Subsequently, gas cooling is turned off until the end of the momentum-conserving phase of the supernova blastwave. This model keeps gas hydrodynamically coupled at all times.

Our feedback model does not explicitly include processes such as cosmic rays, or those caused by young stars such as photoionization, momentum injection from stellar winds, and radiation pressure (e.g., Thompson et al. 2005; Agertz et al. 2013; Booth et al. 2013; Murray et al. 2011; Wise et al. 2012; Hopkins et al. 2012; Simpson et al. 2016; Sharma & Nath 2012; Salem et al. 2016; Farber et al. 2018). Simulations of isolated galaxies by Hopkins et al. (2011) and Hopkins et al. (2012) that included approximations for supernovae, stellar winds, radiation pressure, and photoionization demonstrated that these processes interact non-linearly with one another and that the net effect is difficult to anticipate without self-consistently modeling them together. However, these processes alter the feedback energy injected into the ISM only by a factor of a few. Benincasa et al. (2016) showed that changing the feedback deposited into the ISM by an order of magnitude does not linearly change the SFR. Galaxies self-regulate, with the outward pressure created by feedback balancing the pressure inward due to the gravitational effect of the galaxy’s mass (Ostriker et al. 2010; Kim et al. 2011, 2013; Faucher-Giguère et al. 2013). Thus, simulated star formation is primarily sensitive to how well the vertical structure of the ISM is resolved. Our star formation efficiency is set in combination with our feedback model to match the stellar mass-halo mass relation derived from abundance matching. We show in an upcoming paper that our simulations reproduce realistic sizes at a given stellar mass, as well as gas fractions (Munshi et al., in prep). Hence,

they have roughly the correct surface density and mean ISM pressure, and thus our blastwave supernova feedback drives realistic star formation.

The physical prescriptions described above have been able to reproduce and explain properties of galaxies over a wide range of masses, regardless of which SF recipe is adopted. In addition to simulating the first bulgeless disk galaxy and dark matter cores (Governato et al. 2010; Brook et al. 2011), simulated galaxies match the observed mass – metallicity relation (Brooks et al. 2007; Christensen et al. 2016), the baryonic Tully-Fisher relation (Christensen et al. 2016; Brooks et al. 2017), the size – luminosity relation (Brooks et al. 2011), the stellar mass to halo mass relation determined from abundance matching (Munshi et al. 2013), and the sizes and fractions of HI in local galaxies (Brooks et al. 2017). They also match the abundance of DLA systems

(Pontzen et al. 2008), and the numbers and internal velocities of dwarf Spheroidal satellites (Brooks & Zolotov 2014). In what follows, we extend these successful models to lower masses and demonstrate for the first time that the differing star formation models impact galaxy formation on UFD scales.

Halos are identified and tracked with Amiga’s Halo Finder (AHF Gill et al. 2004; Knollmann & Knebe 2009). AHF calculates the virial mass of each halo (given in this paper by M_{halo}) as the total mass with a sphere that encloses an overdensity relative to the critical density of $200\rho_{crit}(z)$.

3. RESULTS

In this section we highlight the effect of subgrid star formation models on the total number of galaxies predicted in the low halo mass regime.

3.1. *The Formation of Dwarf Galaxies*

Figure 1 shows the cumulative halo mass functions for both of the baryonic (MC and H_2) and dark matter-only versions of the 40 Thieves. The top three lines (solid, dashed, and dotted) include all dark matter halos (both isolated and satellite galaxies) down to $10^7 M_\odot$ in halo mass (corresponding roughly to the hydrogen cooling limit) at $z = 0$, regardless of whether they contain stars. The bottom two lines are only those halos that are “occupied” by stars, and are also shown separately in an inset for clarity. When considering all halos, including halos without stars, it can be seen that there is a discrepancy in the mass functions between the dark matter-only run and the two baryonic versions. The root cause of this mismatch is baryon ejection from low mass halos (either by heating from the UV background and/or as a result of supernova feedback) which slows not only the galaxy growth rate, but the dark matter halo growth rate as well. The overall effect is that a given dark matter halo in a baryonic run is less massive than in the corresponding dark matter-only simulation (see also Sawala et al. 2013; Munshi et al. 2013).

As a direct result, the total number of dark matter halos with $M_{halo} > 10^7 M_\odot$ is reduced ($\sim 75\%$) in the baryonic versions compared to the dark matter-only run.

The inset of Figure 1 shows in closer detail the cumulative halo mass function for only those halos that “host a galaxy,” i.e., contain a minimum of one star particle (see also Sawala et al. 2015) in both the MC and H_2 runs. For the MC run, 14% of halos above $10^7 M_\odot$ are occupied compared to the number of halos in the dark matter-only run, and less than 3% for the H_2 run. That is, there are nearly five times as many occupied halos in the MC run than in the H_2 run. If we focus on only

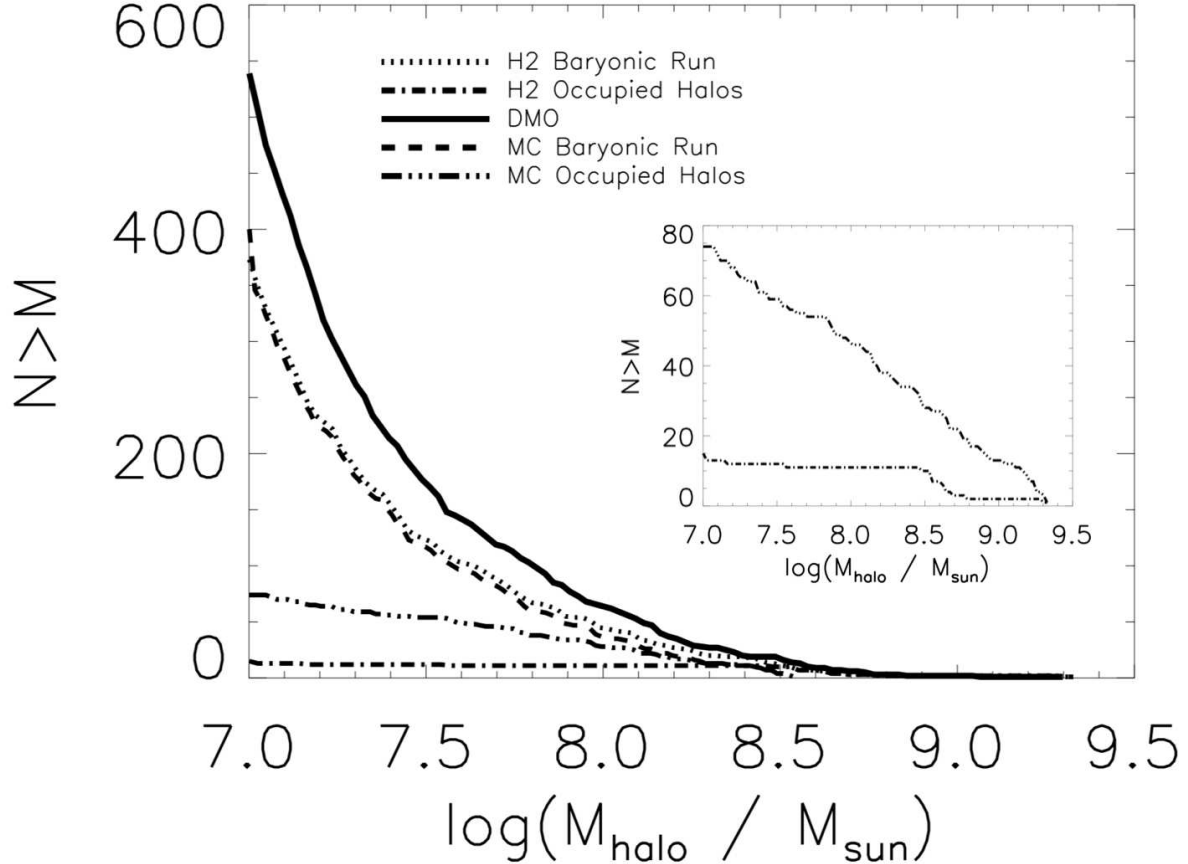


Figure 1. Cumulative halo mass functions. The solid line is the cumulative mass function for the dark matter-only (DMO) run; the dashed and dotted lines are the cumulative mass function for the two baryonic runs using all halos; the two dot-dashed lines are the cumulative mass function using only occupied (luminous) halos in the baryonic runs. Inset: A zoom in of the occupied halos in both the H_2 and MC runs. The fraction of dark (non-luminous) halos continues to increase with decreasing halo mass in the MC run, but remains constant in the H_2 run below $\sim 10^{8.5} M_\odot$ in halo mass. The H_2 run contains far fewer occupied halos than the corresponding MC run, by roughly a factor of five.

those occupied halos where the star formation history (SFH) is “well-resolved” (defined below), this difference drops to about a factor of two (see Figures 2 and 3). The number of luminous halos continues to rise toward lower halo masses in the MC run, but stops rising below $M_{halo} \sim 10^{8.5} M_\odot$ in the H_2 run.

For every dark matter halo that contains a star particle at $z = 0$, we trace back the most massive progenitor halo and identify the time step in which it has the maximum number of dark matter particles. In Figure 2 we show the halo mass and number of star particles inside the halo at that step. Solid lines connect matched galaxies across the MC and H_2 versions of the simulation. For halos above $10^9 M_\odot$, halos are well-matched, with a one-to-one correspondence between formed galaxies. Below $10^9 M_\odot$, however, it is clear that the MC run forms more galaxies than the H_2 run, and even in the matched cases the H_2 galaxies tend to form fewer stars at these low halo masses.

We have examined the $M_{halo,max}$ versus N_{stars} space that contains the H_2 galaxies in Figure 2, i.e., above $10^8 M_\odot$ in maximum halo mass and more than 6 star particles, to test whether their star formation is resolved. In this range, there are MC halos that contain galaxies, but their matched counterparts are completely dark in the H_2 run. We have examined those dark halos in more detail to test whether their lack of star formation is “resolved.” We have approached this in two ways. First, similar to Kuhlen et al. (2013), we compare the surface densities of our gas particles to the critical surface density Σ_{crit} at which atomic H converts to molecular H. The metallicity of our non-star forming gas is $Z/Z_\odot = 10^{-3}$ or lower. At $Z/Z_\odot = 10^{-3}$, $\Sigma_{crit} = 5700 M_\odot \text{ pc}^{-2}$.

The non-star forming gas in the dark matched H_2 halos remains at surface densities $< 10 M_\odot \text{ pc}^{-2}$.

Thus, it would not be capable of forming H_2 , and therefore should not form stars in the H_2 run (see also

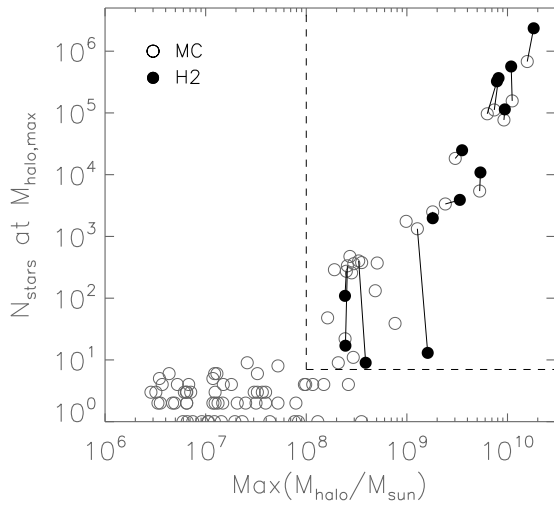


Figure 2. The number of stars in a halo at the time the maximum halo mass is attained versus the maximum halo mass, for both the MC and H₂ runs. The dashed line separates the galaxies that have resolved SFHs ($M_{halo} > 10^8 M_{\odot}$ and ≥ 7 star particles). Lines connect matched galaxies in both the MC and H₂ runs. Above $10^9 M_{\odot}$ in halo masses, the galaxies are well-matched across runs, but below $10^9 M_{\odot}$ there are more galaxies produced in the MC run than the H₂ run.

Sternberg et al. 2014). Second, we can examine the timescale, t_{H_2} , for atomic H to convert to molecular H following Krumholz (2012). Following their equation 7:

$$\frac{t_{H_2}}{t_{ff}} = 24Z^{-1}C^{-1}n_0^{-1/2} \quad (2)$$

where t_{ff} is the free-fall time, Z is the metallicity of the gas relative to solar, C is a clumping factor equal to 10 in our simulations, and $n_0 = \langle n_H \rangle / 1 \text{ cm}^{-3}$ where $\langle n_H \rangle$ is the mean hydrogen density. For the non-star forming gas in our matched H₂ halos, $\langle n_H \rangle$ is about $10 m_H \text{ cm}^{-3}$. The free-fall time depends on $\langle n_H \rangle$ as well, and is 13.6 Myr at $10 m_H \text{ cm}^{-3}$.

Thus, the timescale for H₂ formation, t_{H_2} , is more than 10 Gyr for our gas with $Z/Z_{\odot} = 10^{-3}$. Even at higher densities of $\langle n_H \rangle = 100 m_H \text{ cm}^{-3}$, the timescale for H₂ formation is over 1 Gyr. Thus, significant amounts of H₂ simply cannot form in these halos before reionization begins. We conclude that our dark halos in the H₂ run are behaving as expected, and are “resolved” in their lack of star formation. We therefore take matched halos above $M_{halo,max} = 10^8 M_{\odot}$ and $N_{stars} > 6$ to be resolved in our simulations, and restrict the following analysis to these resolved halos.

By adopting as “resolved” halos in both runs with $M_{halo,max} > 10^8 M_{\odot}$ and $N_{stars} > 6$, it is clear that

we do not mean “converged” across the two star formation recipes. The star formation in the two runs in the lowest mass halos is dramatically different, with the MC run forming stars while matched halos in the H₂ run remain dark. Even when the H₂ run forms stars there is a discrepancy in stellar mass with the matched halos in the MC run for halos with $M_{halo,max} \lesssim 10^9 M_{\odot}$. This is exactly the difference we wish to explore in this work.

In Figure 3 we show the resulting stellar mass to halo mass relation for resolved halos in both the MC (left panel) and H₂ (right panel) versions of the 40 Thieves. Each galaxy is color coded by its V -band magnitude at $z = 0$. Filled circles are central (isolated) galaxies, while stars are satellite galaxies. Four of the lines show results from abundance matching in dwarf galaxies (Brook et al. 2014; Garrison-Kimmel et al. 2014; Read et al. 2017; Jethwa et al. 2018), and the fifth line shows the simulation results of Sawala et al. (2015). The stellar masses have been calculated following Munshi et al. (2013), based on photometric colors. To be consistent with abundance matching, the halo masses are the mass in the corresponding dark matter-only run. Note that we plot $z = 0$ halo masses, while the abundance matching results use maximum halo mass. Thus, the satellite results should not be compared directly to the lines (though we note that all satellites must have peak halo masses above $10^8 M_{\odot}$ to be included in the well-resolved sample shown here).

Again, it is immediately obvious from Figure 3 that there are a set of galaxies residing in halos above $M_{halo} \sim 10^9 M_{\odot}$ that are produced in both runs. However, below $\sim 10^9 M_{\odot}$ the number of galaxies diverges, with twice as many halos containing galaxies in the MC run. We can now see from Figure 3 that many of these low mass halos are satellites (colored stars). There are five times as many satellites in the MC run than in the H₂ run.

All of the satellites in these runs are in the ultra-faint luminosity range. Like observed UFDs (Brown et al. 2012, 2014; Weisz et al. 2014a,b), they tend to form the bulk of their stars early, with their star formation trickling off soon after reionization (see Figure 5, discussed further below). Thus, in Figure 4 we compare the phase diagram for gas that forms stars within the first 1 Gyr of both simulations (i.e., before the end of reionization at $z \sim 6$). Although there is some overlap in the star formation temperatures and densities between the two runs, there is a clear offset in the regions where the majority of stars form. In the MC run (grey points), stars tend to form from gas that spans a range of temperatures (up to 10^4 K) but is near the threshold density ($100 m_H \text{ cm}^{-3}$). In the H₂ run (contours and black

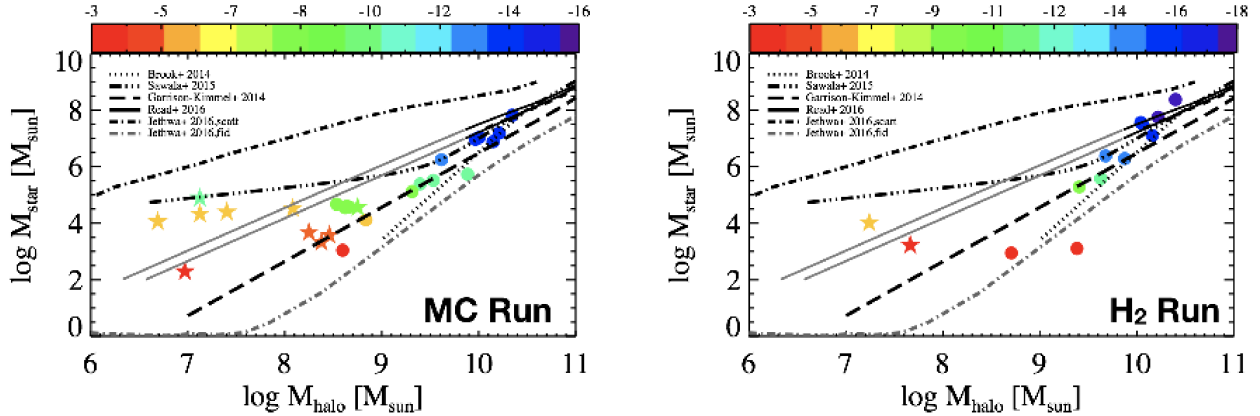


Figure 3. Stellar to Halo Mass relationship for both simulations, showing only the converged galaxies from Figure 2. *Left panel:* MC Run. *Right panel:* H₂ run. Circles are central galaxies and stars are resolved satellites. Galaxies are color-coded by their V-band magnitude (see color bar on top). Stellar masses are derived based on photometric colors, and halo masses are taken from the DM-only version of the run to be consistent with the abundance matching results shown (Brook et al. 2014; Garrison-Kimmel et al. 2014; Read et al. 2017; Jethwa et al. 2018). We plot $z = 0$ halo masses. We also show simulation results from Sawala et al. (2015). A similar number of central galaxies form in both simulations for $M_{\text{halo}} > 10^9 \text{ M}_{\odot}$, but more galaxies form in the MC run at lower halo masses, and there are many more luminous satellites in the MC run.

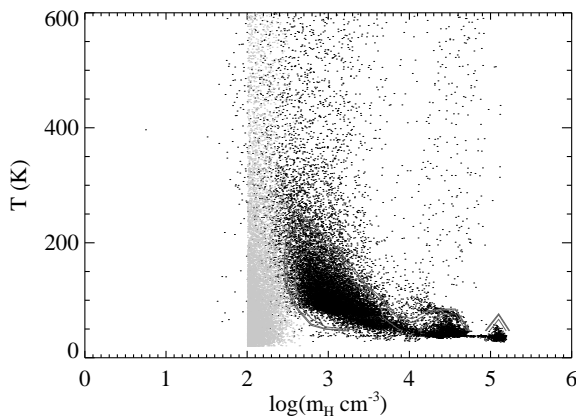
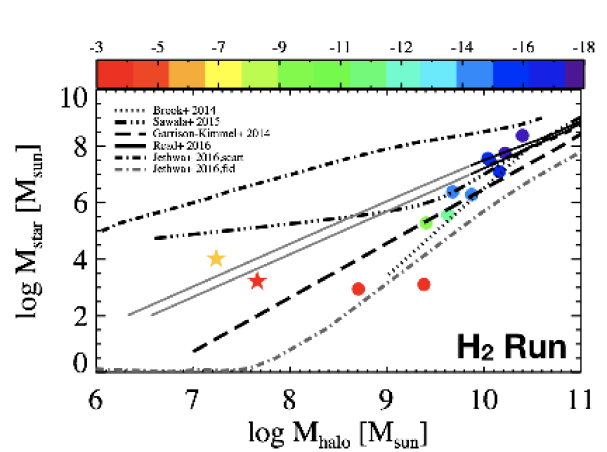


Figure 4. Comparison of the phase diagrams for star forming gas between the MC run (grey points) and the H₂ run (contours + black points) for all stars formed in the first Gyr of the simulation. Note that the range of densities forming stars in the H₂ run, while slightly overlapping with that in the MC run, overwhelmingly tend to be higher than those in the MC run.

points), star-forming gas forms from colder, denser gas ($< 500 \text{ K}$ and $\gtrsim 1000 \text{ m}_H \text{ cm}^{-3}$). This difference was also discussed in CH12 (see their Figure 13).

The higher densities that stars form from in the H₂ model is tied directly to the subgrid H₂ formation model. As described in CH12, when metals are present the formation of H₂ is dominated by formation on dust grains. In the reionization epoch when metallicities are extremely low, formation may also proceed through gas-phase reactions. However, during the reionization epoch



both of these processes are inefficient and slow, as previously discussed in this section. As a result, gas particles will frequently reach high densities through gravitational collapse prior to forming significant amounts of H₂. At the same time, the low metallicities reduce the amount of dust-shielding, which means that H₂ (and thus star formation) can only persist in high density gas. For most of the H₂ subhalos, significant amounts of H₂ can never be created before reionization removes the gas from the halos. In the MC run, because stars can form in lower density atomic gas, star formation can begin before reionization quenches the satellites. This also explains why the MC run tends to form more stars in general for galaxies in halos with $M_{\text{halo}} < 10^9 \text{ M}_{\odot}$ (see Figure 2).

The slow H₂ formation time scales and the reduced dust-shielding at low-metallicity are the primary drivers of the differences in star formation. At solar metallicities, the two models form star particles at similar densities, but the models diverge as metallicity decreases. As we have found here, the effect of metallicity is strongest at high- z in the smallest dwarf galaxies, because this is where metallicities are lowest. In these halos, low metallicities make H₂ slow to form (more than 1 Gyr, as calculated above) and the gas must reach very high densities in order to shield H₂. This delay means that reionization is able to stop star formation before it begins, or soon thereafter for the simulation with H₂ star formation, in contrast to the MC run.

The sensitivity to reionization suggests that our results may be dependent on reionization model. Reionization is expected to leave a visible imprint on the satel-

lite luminosity function in the UFD range (Bose et al. 2018). We have adopted the same model in both simulations, following Haardt & Madau (2012). However, Haardt & Madau (2012) has been shown to heat the IGM earlier ($z \sim 15$) than it should (Oñorbe et al. 2017), making the impact of reionization particularly strong on our results. We leave it to future work (Applebaum, in preparation) to quantify the impact of a gentler reionization model on the formation of ultra-faint dwarf galaxies, and restrict the focus of this paper to the role of star formation recipe alone.

Even at $z = 0$, the most massive matched dwarfs in this work still show a difference in the effective star formation density threshold due to the impact of metallicity on dust-shielding (CH12; Christensen et al. 2014b). Despite this, dwarf galaxies in halos above $\sim 10^9 M_{\odot}$ generally still form similar numbers of star particles, due to their ability to self-regulate. This is consistent with the prior results discussed in the Introduction that found that the density threshold had little impact on the resulting SFR. However, a slight excess of stars seems to form in the H_2 model relative to the MC model at these masses (see Figure 2). This excess is likely due to the ability of the gas to shield in the H_2 model, protecting the gas from heating and leading to additional cold gas present in the H_2 simulations. The excess cold gas results in slightly higher stellar masses in the H_2 run in halos $\sim 10^{10} M_{\odot}$.

Kuhlen et al. (2012) were the first to show that a model for H_2 -based star formation could suppress star formation in dwarf galaxies primarily due to their lower metallicities, but the specific results of their model are quite different than ours. They found that their H_2 model suppressed all star formation in halos below about $M_{halo} = 10^{10} M_{\odot}$, while our H_2 model forms stars in halos down to $M_{halo} = 10^{8.5}$. The H_2 formation and destruction model in Kuhlen et al. (2012) is quite different than we use here. For example, they do not explicitly follow destruction by Lyman-Werner radiation from young stars, but rather assume a two-phase ISM with a warm and cold neutral component that should balance formation of H_2 with destruction. They also adopt a metallicity floor imposed on their gas at high z but do not include metal mixing, and they show that the exact lower mass halo that can form stars is resolution dependent (see their figure 16). Our H_2 model, on the other hand, is not resolution dependent as long as the simulation can resolve high density peaks above $100 m_H \text{ cm}^{-3}$ (see CH12). Thus, the effect that we are seeing in this work is quite different than in Kuhlen et al. (2012). Reionization played no role in that work, since their lowest mass halo that was able to form stars was

well above the halo mass thought to be impacted by reionization. On the other hand, the changes in stellar mass that we see in halos below $\sim 10^9 M_{\odot}$ are explicitly due to the fact that these are halos in which reionization can strongly affect the evolution. The MC halos are able to start forming stars at lower densities than their H_2 counterparts, and thus are able to produce more stars before reionization removes their gas.

3.2. Delayed Merging

Early star formation is not the only reason why there are more satellites in the MC run than in the H_2 run: more of the satellites survive. Three of the surviving subhalos in the MC run are completely disrupted in the H_2 run after merging with a parent halo. Two of those halos had managed to form stars in the H_2 run before being fully destroyed. In fact, a close examination of Figure 5 shows that there is a surviving satellite in the MC run with a very extended SFH (boldest red dashed line in the left panel). This satellite had a counterpart in the H_2 run with an extended SFH, but the subhalo is completely disrupted and part of the second largest halo in the H_2 run at $z = 0$.

Schewtschenko & Macciò (2011) showed that mergers occur later in simulations with baryonic feedback than in matched halos in an identical dark matter-only simulation. They hypothesized that the pressure of the hot halos found in baryonic simulations slows down accretion of subhalos. Our simulated dwarf galaxies *do* have hot halos of gas around them (Wright et al. 2018), with the mass in hot gas being twice as much to more than an order of magnitude higher than the HI gas mass. Importantly, later infall of subhalos leads to less tidal mass loss for subhalos around baryonic dwarf galaxies simply due to the fact that there is less time for tidal stripping between infall and $z = 0$ (Ahmed et al., in prep.). The end result should be that fewer satellites are fully destroyed at $z = 0$ for a run with baryonic feedback.²

These results suggest that the feedback in the MC run is stronger, delaying mergers of subhalos. Indeed, another indication that feedback is stronger in the MC run is that the overall halo masses tend to be lower (see comparison of maximum M_{halo} for matched halos in Figure 2). As mentioned previously, feedback reduces the growth of halos (Munshi et al. 2013; Sawala et al. 2013). Despite the fact that the feedback recipe is the same in

² This assumes that additional tidal effects from the potential of the central galaxy are negligible. The disk potential is not negligible in Milky Way-mass galaxies (Peñarrubia et al. 2010; Zolotov et al. 2012; Arraki et al. 2014; Brooks & Zolotov 2014; Garrison-Kimmel et al. 2017b), but is expected to be negligible in dwarf galaxies.

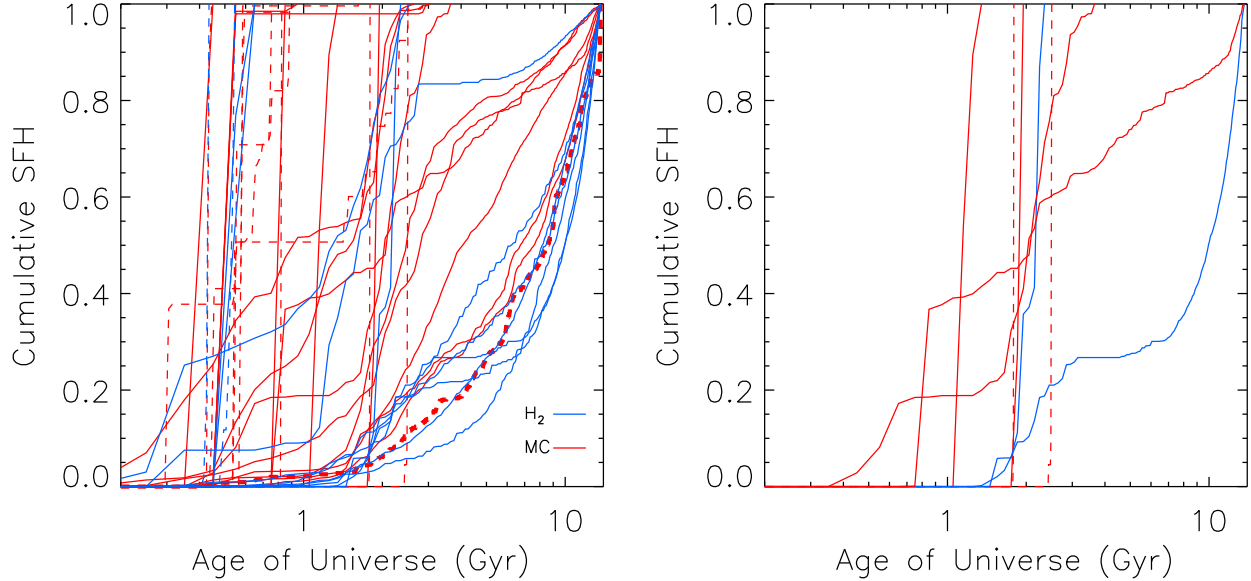


Figure 5. Cumulative SFHs for the simulated galaxies. The MC run is shown in red, the H_2 run in blue. Solid lines are central galaxies at $z = 0$, while dashed lines are satellites. *Left Panel:* All surviving resolved galaxies at $z = 0$. One MC satellite is shown in a thicker dashed line that has an extended SFH, but its H_2 counterpart has been destroyed in a merger, as discussed in Section 3.2. *Right Panel:* A subset of the galaxies shown in the left panel that are discussed in Sections 3.2 and 4.1. The four MC galaxies that do not begin forming stars until after 1 Gyr are shown (two satellites – red dashed, two centrals – solid red). The two H_2 galaxies that don't start star formation until after 1 Gyr are shown (solid blue) along with their MC counterparts that start forming stars much earlier (solid red).

both the MC and H_2 runs, feedback is injected into lower density gas in the MC run because the MC run rarely reaches the higher densities found in the H_2 run (see, e.g., figure 7 of Christensen et al. 2014b). When comparing the nine most massive isolated dwarfs at $z = 0$ (where the stellar masses are similar), the H_2 dwarf galaxies on average have 10% higher dark matter mass and more than twice the mass in hot gas within their virial radii (and more baryons generally) compared to their MC counterparts. Thus, it seems that the MC galaxies have been able to remove more baryonic material from their halos, delaying their growth in dark matter as well.

However, this result is seemingly at odds with previous comparisons of these two models (Christensen et al. 2014a), which found that the H_2 model had more effective feedback and drove slightly more outflows. While the previous work used the GASOLINE code, we use ChaNGa with an updated SPH treatment (Wadsley et al. 2017) and quantized feedback. It is not clear if these changes alter the feedback, making the MC run more effective at removing baryons. A full investigation is beyond the scope of this paper, but we find that all evidence points to stronger feedback in the current MC runs than in the H_2 runs.

Since the hot gas mass of the MC galaxies is smaller than the H_2 runs, the delayed merging of subhalos does not seem to be a direct result of pressure from the hot halo (as was proposed in Schewtschenko & Macciò 2011), but rather a response to the ejection of the gas itself.

We will investigate this further in future work (Ahmed et al., in prep.). We note that all three of the surviving subhalos in the MC run are completely merged in the dark matter-only run as well.

In summary, these results suggest that feedback can lead to delayed mergers of the UFD satellites. Combined with the ability to form stars at early times in more halos in the MC run, this makes the difference in satellite numbers even more stark at $z = 0$ between the two runs.

4. IMPLICATIONS

The fact that star formation is restricted to different types of gas in these two commonly adopted models leads to some implications that should be considered when comparing predictions from different simulations.

4.1. Delayed Star Formation

Consistent with the results presented in Section 3, we find that there is a delay in the onset of star formation in the H_2 run compared to matched halos in the MC

run. We highlight a few cases of this in the right panel of Figure 5. In general (as can be seen in the left panel of Figure 5), most of our galaxies begin to form stars before $z = 6$, i.e., in the first 1 Gyr after the Big Bang. However, there are two (central) galaxies in the H_2 run that only begin to form stars after 1 Gyr (shown in blue). Because their counterparts in the MC run can form stars without first generating significant amounts of H_2 , the MC counterparts all begin star formation before the end of reionization (the counterparts are also shown in red in the right panel of Figure 5 – they are the two MC galaxies shown that begin star formation before 1 Gyr).

However, post-reionization onset of star formation cannot be attributed to only a single star formation model. There are four galaxies (two centrals and two satellites, shown in the right panel of Figure 5) in the MC run that do not begin to form their stars until after 1 Gyr. In each of the four cases, their counterparts in the H_2 run are dark halos that never formed stars. In that case, we might say that the star formation is so delayed in the H_2 run that it does not occur before $z = 0$.

Thus, in both models we see a few galaxies that delay the start of their star formation until after reionization, meaning that the starting time of star formation cannot be used to discriminate the models. While the H_2 run has consistently later star formation (or none at all by $z = 0$) compared to matched galaxies in the MC run, there is no obvious trend in onset time that could be used to discriminate models based on observations. Rather, it is the number of galaxies and stellar mass of those galaxies that discriminates the models (discussed in the next section).

In general, all observed galaxies have early star formation, though the error bars on the time of onset can be 1 Gyr or more depending on how far down the main-sequence resolved stars are detected (Brown et al. 2012, 2014; Weisz et al. 2014a,b). It is not clear if our galaxies that delay star formation until after reionization are consistent with observations. However, the dwarf galaxies in these simulated volumes are much further away from a massive galaxy than any observed galaxies with resolved star formation histories that have pushed below the oldest main-sequence turnoff. Our dwarf galaxies are ~ 5 Mpc away from a Milky Way-mass galaxy. It remains to be seen if environment plays any role in onset of star formation (Applebaum et al., in prep).

4.2. Stellar Mass Function

The factor of two difference in the number of faint dwarf galaxies that form between our two models will lead to different faint ends of the stellar mass func-

tion (SMF). Additionally, the fact that the MC run forms higher stellar masses for matched galaxies with $M_{halo,max} < 10^9 M_\odot$ (see Figure 2) will also alter the SMF.

In this section we demonstrate the difference in SMF that should arise due to these effects.

First, we demonstrate the difference in the SMF that arises due to the different number of low mass galaxies in each model alone. For both the MC and H_2 models, we populate a SMF following the method outlined in Garrison-Kimmel et al. (2017a) in which the scatter, σ , in the stellar mass at a given halo mass grows as

$$\sigma = 0.2 + \gamma(\log_{10}M_{\text{halo}} - \log_{10}M_1) \quad (3)$$

where γ is the rate as which the scatter grows, and M_1 is a characteristic halo mass above which the scatter remains constant. We adopt the scatter model for field galaxies from Garrison-Kimmel et al. (2017a), where $M_1 = 10^{11.5} M_\odot$ and $\gamma = -0.25$. We populate the $z = 0$ ELVIS catalogs (Garrison-Kimmel et al. 2014) with this SMHM relation, and then assign galaxies as “dark” based on the fraction of luminous to non-luminous halos shown in Figure 1 for each of our models. The resulting SMFs are shown in

Figure 6 as the blue (MC) and green (H_2) lines. We do this 1000 times in order to estimate our errors (dashed lines), and normalize the results so that each has 12 galaxies with stellar mass comparable to Fornax (this is roughly the number of Fornax-mass galaxies within 1 Mpc McConnachie 2012). Figure 6 demonstrates that there is a difference in slope below $M_{\text{star}} \sim 10^5 M_\odot$, with the H_2 simulation predicting the shallower faint-end slope.

The blue and green lines adopt the same slope and scatter of the SMHM relation, and thus only reflect the change in the fraction of “occupied” dark matter halos shown in Figure 1. However, the H_2 model tends to form fewer stars in matched halos at the low mass end, which will yield a steeper SMHM slope that will impact the SMF. As can be seen in Figure 3, the Garrison-Kimmel et al. (2017a) SMHM slope appears to be a decent fit to the central galaxies in the MC run (left panel). However, the Brook et al. (2014) SMHM slope appears to be a better match to the central galaxies in the H_2 run. Our simulations do not have enough galaxies to independently define the slope and scatter of the SMHM relation for each prescription, so we adopt the slope and scatter of Garrison-Kimmel et al. (2017a) to describe the MC run, and Brook et al. (2014) to describe the H_2 run, in order to show the additional effect that the steeper SMHM relation will have on the SMF. We assume the same growing scatter as in

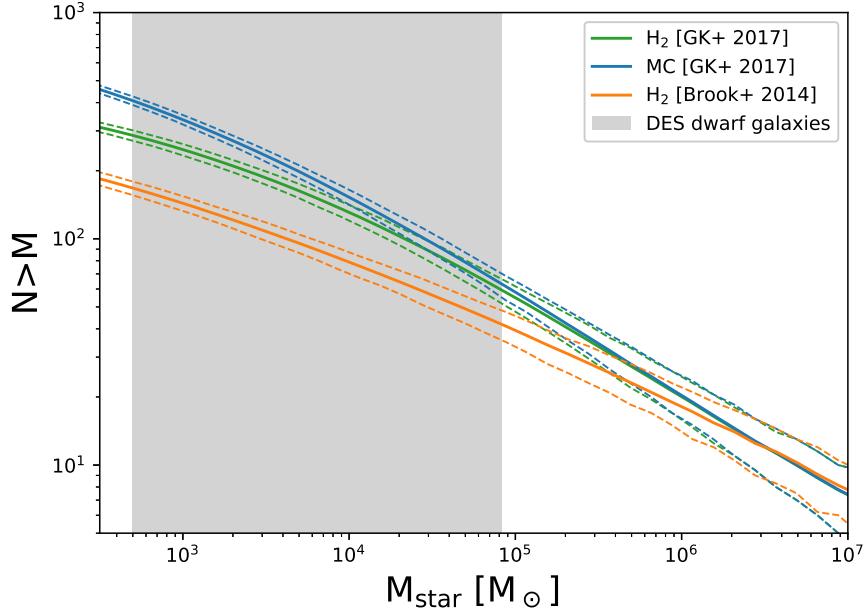


Figure 6. Comparison of stellar mass functions predicted by the H_2 run (green) and the MC run (blue) assuming the slope and scatter of the SMHM relation follows Garrison-Kimmel et al. (2017a) and following the occupation fractions shown in Figure 1. The orange line is the SMF predicted for the H_2 run assuming the slope of the SMHM better follows Brook et al. (2014). The grey shaded region represents the recent discovery space for DES. 1- σ errors for each mass function are shown in corresponding colored dashed lines.

the Garrison-Kimmel et al. (2017a) relation but applied to the Brook et al. (2014) slope, and again adopt the galaxy occupation fraction for the H_2 simulation. The result is shown as the orange line in Figure 6. It can now be seen that there is a dramatic difference in the number of expected UFD galaxies in the two models.

The SMF for the two runs is indistinguishable above $M_{star} \sim 10^5 M_\odot$. Since this is the mass range that is currently best constrained, current observations cannot constrain the two models. However, galaxies at lower stellar masses are currently being discovered by surveys like DES and HSC-SSP, and potentially hundreds will be found near the Milky Way with the *Large Synoptic Survey Telescope* (LSST; Tollerud et al. 2008; Walsh et al. 2009; Newton et al. 2018), and out to greater distances using integrated light surveys (Danieli et al. 2018). The masses of the UFDs discovered in DES is highlighted by the grey region in Figure 6. It can be seen that pure number counts of faint dwarfs in LSST (i.e., UFDs found out to ~ 1 Mpc) can help us to constrain how star formation proceeded at high redshift.

4.3. Satellites of Dwarf Galaxies

As discussed above, the MC simulation contains five times more satellites than the H_2 run at $z = 0$. Here we use this result to estimate the predicted frequency of

satellites around dwarfs in the Local Group in the two models.

We follow the methodology presented in Wheeler et al. (2015) and use the ELVIS suite of collisionless zoom-in simulations of Local Group-like environments (Garrison-Kimmel et al. 2014) combined with the results of our two simulations to predict the frequency of a satellite around a dwarf galaxy with $M_{vir} \sim 10^{10} M_\odot$. To summarize the procedure: (1) we select isolated dwarf galaxies from the ELVIS suite from both the isolated and paired Milky Way-mass halo simulations and (2) we estimate the frequency of subhalos with peak $M_{vir} \geq 10^8 M_\odot$ within 50 kpc of the dwarf host, as appropriate for our work since this is the lowest (maximum) halo mass that we consider resolved. The detailed methodology can be found in Wheeler et al. (2015), which we directly follow in order to compare results. Figure 7 shows the results.

As expected, the MC model predicts that UFD satellites of dwarf galaxies are more abundant than the H_2 model. The MC run produces non-negligible frequencies for finding at least one satellite around a dwarf host, predicting 46% of isolated dwarfs above our mass threshold should have at least one luminous satellite. The H_2 model also predicts UFD satellites will be somewhat common, but roughly a factor of 4 less frequent with 16% of isolated dwarfs hosting a UFD satellite. The

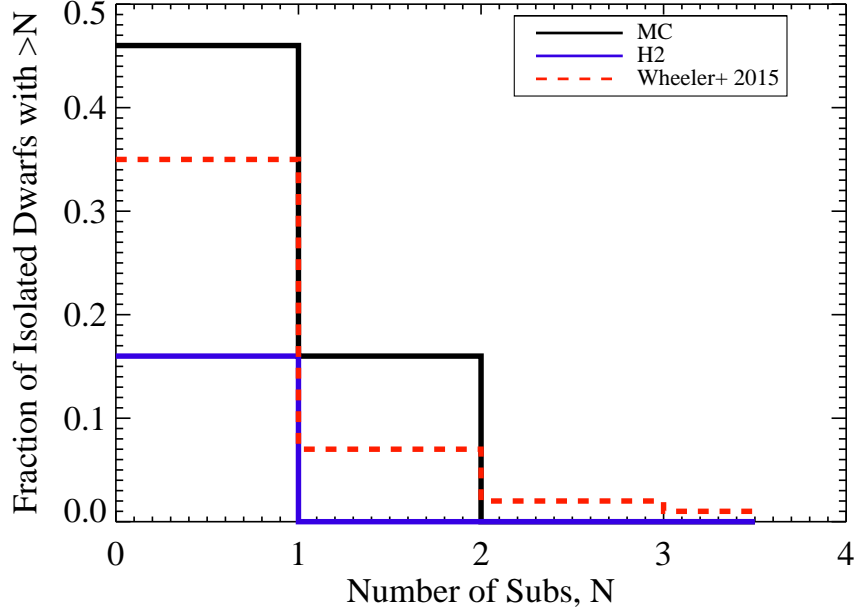


Figure 7. Comparison of the predictions from hydrodynamic simulations for the number of luminous subhalos around dwarf galaxies. The two solid lines are for the simulations in this work (black = MC model, blue = H_2 model), the red dashed for Wheeler et al. (2015). Each simulation has a different star formation and/or feedback recipe, with the model in Wheeler et al. (2015) being more similar to the MC run (discussed further in the text). This figure demonstrates that the subgrid physics of the simulation affects the predictions for luminous subhalos, in some cases by a factor of ~ 4 .

H_2 model also suppresses galaxy formation to the point that no Local Group dwarf with $M_{vir} \sim 10^{10} M_\odot$ is expected to host more than one luminous satellite companion, while multiple UFD satellites are infrequent but possible in the MC run.

The two simulations in this work differ in star formation prescription, but not feedback recipe. On the other hand, the Wheeler et al. (2015) results adopt the FIRE 1 star formation and feedback prescription (Hopkins et al. 2014). FIRE 1 adopted a threshold for star formation of $> 100 m_H \text{ cm}^{-3}$, while the updated FIRE 2 adopts a higher density threshold of $> 1000 m_H \text{ cm}^{-3}$ (Hopkins et al. 2018). Both FIRE 1 and FIRE 2 use the equilibrium model from Krumholz & Gnedin (2011) to determine the H_2 fraction in a given particle, which is used to calculate the self-shielding of the gas particle and the cooling rate. The presence of H_2 for star formation is an explicit requirement, which is usually ensured by the simultaneous requirement of a high density threshold. However, because FIRE adopts the equilibrium model of H_2 , there is no delay in star formation due to the H_2 formation time.

Figure 7 demonstrates that the predictions in Wheeler et al. (2015) are closer to our MC results than H_2 results. This is in line with our expectations given the similarity in star formation threshold (and resolution) between the

FIRE 1 model and the MC model. Of course, both the feedback and reionization models in FIRE are different than those used here, which may also play some role in the results. We note, though, that we have adopted a reionization model (Haardt & Madau 2012) that is known to lead to earlier reionization than that used in FIRE (Faucher-Giguère et al. 2009), as was shown in Oñorbe et al. (2017). Despite the stronger, earlier heating in our MC model, we predict slightly more satellites than Wheeler et al. (2015). This allows us to place a lower limit on the errors on our predictions of at least $\sim 10\%$.

The results presented in Figure 7 serve to underscore that current predictions for the number of UFD satellites expected around Local Group dwarfs should be approached with caution. This work highlights the range of values we expect to see in state-of-the-art zoom simulations that reach the UFD mass/luminosity range. However, we do not currently know what star formation physics model is “correct.” Until future observations better constrain the models, we must find independent constraints from existing observations.

We note that we do not have an LMC-mass galaxy in this simulation volume. The halo mass of the LMC is estimated to be at least $M_{halo} > 10^{11} M_\odot$ (Besla 2015; Dooley et al. 2017a; Peñarrubia et al. 2016;

Laporte et al. 2018). A lot of work has been done recently to determine if the DES dwarfs are satellites of the LMC or Magellanic System (e.g., Deason et al. 2015; Jethwa et al. 2016; Sales et al. 2017). The majority of studies find that 25-50% of the newly discovered DES dwarfs are likely to have come in with the Magellanic Clouds. Kallivayalil et al. (2018) and Pace & Li (2018) derive proper motions from *Gaia* data to test whether the UFD satellites have kinematics consistent with falling in with the Clouds. Between the two studies, seven UFDs are thought to be associated. It is not immediately clear if these high numbers are compatible with our predictions, given our lack of LMC-mass galaxies.

The models of Dooley et al. (2017a) predict \sim 5-15 UFDs with $M_{star} > 3000 M_{\odot}$ (the lower limit for at least seven star particles in our “resolved” galaxies) around an LMC-mass galaxy, and \sim 2-9 around an SMC-mass galaxy. These results are consistent with the number of UFDs that are potentially associated with the Magellanic Cloud system. However, the abundance matching results of Dooley et al. (2017b) put the SMC in a halo with $M_{halo} > 10^{11} M_{\odot}$, more massive than our most massive simulated galaxy. Based on their abundance matching results, a more direct comparison of our most massive simulated galaxies is to WLM, for which Dooley et al. (2017b) expect to find roughly one UFD companion. This suggests that our results are generally consistent with the estimates in Dooley et al. (2017b,a), as they should be as long as our simulation results are reasonably described by one of the SMHM relations that they explore. However, it is unlikely that even our MC model would predict seven satellite companions around an LMC-mass galaxy. To reach such high numbers, the satellites must be associated with the whole Magellanic system (SMC+LMC), rather than just the LMC.

If the large number of candidate DES satellites really did fall in with the Magellanic Clouds, another way to reconcile it with our results would be to allow galaxy formation to occur down to lower mass halos than we use here ($10^8 M_{\odot}$ in peak halo mass). Jethwa et al. (2018) found that restricting the fraction of subhalos with peak halo masses of $10^8 M_{\odot}$ to less than 10% would underpredict the number of observed UFD galaxies. This suggests that galaxies should form in halos at least down to this mass. On the other hand, Tollerud & Peek (2018) suggest that reionization prevents galaxy formation in halos below $3 \times 10^8 M_{\odot}$ in peak halo mass. Their model is simple, with a sharp transition that has all halos hosting galaxies above this mass and none below it. This behavior is actually quite similar to our H_2 model. Thus, the observational data currently suggest that either of

our models (with galaxies forming in peak halo masses above $10^8 M_{\odot}$) is in reasonable agreement with the data.

We leave it to future work to examine LMC mass galaxies and their satellite populations in more detail.

5. DISCUSSION

In this work, we have found that there is a significant delay in star formation and reduction in overall efficiency of star formation in simulated UFD galaxies when adopting a non-equilibrium H_2 -based star formation prescription relative to a prescription that adopts a commonly-used temperature-density threshold. The reduction in star formation in the H_2 model is due the long formation times of H_2 at low metallicities in low mass halos. The delay in H_2 formation prevents or suppresses star formation in UFD galaxies because reionization can heat their gas before significant star formation can occur. In contrast, the MC model allows star formation to occur as soon as gas reaches a high enough density threshold, and more stars form before reionization can remove the gas.

We want to emphasize that it is unclear if either of the explored models, MC or H_2 , is “correct.” The MC model does not take into account whether the gas can shield when forming stars, and shielding of the gas is likely to be a necessary ingredient for star formation to occur. Similarly, it has been argued that H_2 is not necessary for star formation, but that its presence is correlated with the ability of the gas to shield (Glover & Clark 2012; Mac Low & Glover 2012; Krumholz et al. 2011; Krumholz 2012; Clark & Glover 2014). Hence, it is possible that neither model accurately reflects the physics of star formation in the first halos. Instead, a model that links star formation to shielding may be more appropriate (Byrne et al., in prep.)

We also emphasize that not all H_2 models for star formation will behave in the same way as our adopted non-equilibrium H_2 model. As discussed in the Introduction, some H_2 models assume equilibrium between the formation and destruction of H_2 in the interstellar medium. Because H_2 formation is not explicitly followed, there will be no dependence on the formation time of H_2 in equilibrium models. Thus, equilibrium H_2 models may behave more like the MC model, though this remains to be tested.

Our goal in this paper is not to figure out which model is correct. Rather, our goal is to stress the need for caution in interpreting simulated UFD results. As simulations push to ever-higher resolution and UFDs begin to be modeled for the first time in fully cosmological simulations run to $z = 0$, the predictions for UFDs are likely to vary from model to model due to the assumptions

adopted for star formation by varying modelers. This is in contrast to model predictions in the classical dwarf galaxy mass range because classical dwarf galaxies are capable of self-regulating their star formation, reducing dependency on the adopted prescriptions in their resulting stellar masses. As we push into the UFD mass range, we are simulating galaxies for the first time that can no longer self-regulate.

However, we have highlighted a few future observables that will help to pinpoint the conditions for star formation in the first low mass halos. Specifically, we have shown that the SMF and the number of UFD satellites around classical dwarf galaxies will be strongly impacted by star formation in UFDs during the reionization epoch. A better constraint on the slope and scatter of the SMHM relation at low masses will also help to constrain the models.

6. SUMMARY

In this work, we have used the highest resolution simulations to date of a cosmic volume of dwarf galaxies in order to examine the effect of star formation recipes on the formation of UFDs. We run our volume with two different star formation recipes that are common in the literature: one with a temperature/density threshold for star formation, and another that requires the presence of H_2 for star formation. The main differences that manifest between the two models occur in extremely low metallicity gas and are 1) the timescale over which star formation takes place and 2) the effective gas densities at which star particles form (the first above $100 \text{ } m_H \text{ cm}^{-3}$ and the H_2 primarily above $1000 \text{ } m_H \text{ cm}^{-3}$ due to gravitational collapse during H_2 formation and reduced dust shielding). We find that these differences lead to drastically different results for galaxy formation in halos with $M_{vir} < 10^9 \text{ M}_\odot$.

Broadly, the ability of the stars in the MC model to form earlier leads to more galaxies that can form in low mass halos. When the H_2 dependency is introduced into the star formation model, however, gas in low-metallicity, low-mass halos is less likely to reach significant molecular fractions prior to reionization and gas may never reach densities high enough for dust-shielding to allow for substantial H_2 . As a result, many fewer low-mass halos in the H_2 run produce stars. Even when they do produce stars, they form substantially less than their matched counterparts in the MC run, leading to a steeper SMHM relation and shallower faint-end SMF. Since these stars tend to form in the reionization epoch, the exact model for reionization is likely to impact these results. In this work, we have adopted a strong feedback model in both cases, [Haardt & Madau \(2012\)](#). In future

work (Applebaum et al., in prep.), we will explore the role of reionization in setting the number of UFD galaxies that form around a Milky Way-mass galaxy.

For the two models that we examine here, we find twice as many resolved galaxies form in the lower threshold (MC) run. However, most of these are satellites. We also find that more satellites *survive* in the MC run, and we conjecture that feedback in the satellites somehow contributes to the delayed mergers/disruption of these satellites. The combined effect leads to five times as many satellites in the MC run than in the H_2 run.

We have convolved our results with the halos in the ELVIS simulation suite ([Garrison-Kimmel et al. 2014](#)) in order to make predictions for the number of UFD satellites around Local Group dwarf galaxies. We find that the MC model predicts four times as many dwarfs should host at least one luminous satellite compared to the H_2 model, while the H_2 model predicts that no Local Group dwarfs should host more than one UFD satellite, and only $\sim 15\%$ should host just one UFD. Our MC model produces a similar prediction to that of [Wheeler et al. \(2015\)](#), where the density threshold for star formation was also $100 \text{ } m_H \text{ cm}^{-3}$.

Our results also have implications for additional observables. We show that the predicted SMF that can be probed by LSST is shallower in the UFD range for the model that restricts star formation to gas that has H_2 . This suggests that pure number counts of UFDs that we discover in the future can help to pinpoint the conditions required for the first star formation in low mass halos.

In future work, we will use additional simulation volumes that yield a statistical sample of simulated dwarfs to further examine the observational implications presented in this paper. We will study the effects of varying reionization models, take a closer look at the numbers of satellites in a Milky Way-mass halo that might have fallen in as associations, study dwarfs in groups and clusters,

and quantify the predicted number of dwarf galaxies as a function of radius that LSST might discover. This work is just a first step, highlighting the need to push theoretical work in the ultra-faint regime, as future observations push to become complete in this mass range. We have demonstrated here that $z = 0$ UFDs can provide clues to understanding the high- z universe.

The authors would like to thank Sarah Loebman, Jillian Bellovary, and Dan Weisz for useful discussions relating to this paper. FDM acknowledges funding from the VIDA fellowship. AMB and FDM acknowledge support from HST-AR-13925. Resources supporting this

work were provided by the NASA High-End Computing (HEC) Program through the NASA Advanced Supercomputing (NAS) Division at Ames Research Center. This research is part of the Blue Waters sustained-petascale computing project, which is supported by the

National Science Foundation (awards OCI-0725070 and ACI-1238993) and the state of Illinois. Blue Waters is a joint effort of the University of Illinois at Urbana-Champaign and its National Center for Supercomputing Applications. This work was supported by a PRAC allocation NSF award number OCI-1144357.

REFERENCES

Abel, T., Bryan, G. L., & Norman, M. L. 2002, *Science*, 295, 93, doi: [10.1126/science.295.5552.93](https://doi.org/10.1126/science.295.5552.93)

Agertz, O., & Kravtsov, A. V. 2016, *ApJ*, 824, 79, doi: [10.3847/0004-637X/824/2/79](https://doi.org/10.3847/0004-637X/824/2/79)

Agertz, O., Kravtsov, A. V., Leitner, S. N., & Gnedin, N. Y. 2013, *ApJ*, 770, 25, doi: [10.1088/0004-637X/770/1/25](https://doi.org/10.1088/0004-637X/770/1/25)

Anderson, L., Governato, F., Karcher, M., Quinn, T., & Wadsley, J. 2017, *MNRAS*, 468, 4077, doi: [10.1093/mnras/stx709](https://doi.org/10.1093/mnras/stx709)

Arraki, K. S., Klypin, A., More, S., & Trujillo-Gomez, S. 2014, *MNRAS*, 438, 1466, doi: [10.1093/mnras/stt2279](https://doi.org/10.1093/mnras/stt2279)

Barnes, J., & Efstathiou, G. 1987, *ApJ*, 319, 575, doi: [10.1086/165480](https://doi.org/10.1086/165480)

Bechtol, K., Drlica-Wagner, A., Balbinot, E., et al. 2015, *ApJ*, 807, 50, doi: [10.1088/0004-637X/807/1/50](https://doi.org/10.1088/0004-637X/807/1/50)

Benincasa, S. M., Wadsley, J., Couchman, H. M. P., & Keller, B. W. 2016, *MNRAS*, 462, 3053, doi: [10.1093/mnras/stw1741](https://doi.org/10.1093/mnras/stw1741)

Benson, A. J., Frenk, C. S., Lacey, C. G., Baugh, C. M., & Cole, S. 2002, *MNRAS*, 333, 177, doi: [10.1046/j.1365-8711.2002.05388.x](https://doi.org/10.1046/j.1365-8711.2002.05388.x)

Besla, G. 2015, ArXiv e-prints. <https://arxiv.org/abs/1511.03346>

Bland-Hawthorn, J., Sutherland, R., & Webster, D. 2015, *ApJ*, 807, 154, doi: [10.1088/0004-637X/807/2/154](https://doi.org/10.1088/0004-637X/807/2/154)

Booth, C. M., Agertz, O., Kravtsov, A. V., & Gnedin, N. Y. 2013, *ApJL*, 777, L16, doi: [10.1088/2041-8205/777/1/L16](https://doi.org/10.1088/2041-8205/777/1/L16)

Bose, S., Deason, A. J., & Frenk, C. S. 2018, *ApJ*, 863, 123, doi: [10.3847/1538-4357/aacbc4](https://doi.org/10.3847/1538-4357/aacbc4)

Bovill, M. S., & Ricotti, M. 2011, *ApJ*, 741, 18, doi: [10.1088/0004-637X/741/1/18](https://doi.org/10.1088/0004-637X/741/1/18)

Bromm, V., Coppi, P. S., & Larson, R. B. 2002, *ApJ*, 564, 23, doi: [10.1086/323947](https://doi.org/10.1086/323947)

Bromm, V., & Yoshida, N. 2011, *ARA&A*, 49, 373, doi: [10.1146/annurev-astro-081710-102608](https://doi.org/10.1146/annurev-astro-081710-102608)

Brook, C. B., Di Cintio, A., Knebe, A., et al. 2014, *ApJL*, 784, L14, doi: [10.1088/2041-8205/784/1/L14](https://doi.org/10.1088/2041-8205/784/1/L14)

Brook, C. B., Governato, F., Roškar, R., et al. 2011, *MNRAS*, 415, 1051, doi: [10.1111/j.1365-2966.2011.18545.x](https://doi.org/10.1111/j.1365-2966.2011.18545.x)

Brooks, A. M., Governato, F., Booth, C. M., et al. 2007, *ApJL*, 655, L17, doi: [10.1086/511765](https://doi.org/10.1086/511765)

Brooks, A. M., Papastergis, E., Christensen, C. R., et al. 2017, *ApJ*, 850, 97, doi: [10.3847/1538-4357/aa9576](https://doi.org/10.3847/1538-4357/aa9576)

Brooks, A. M., & Zolotov, A. 2014, *ApJ*, 786, 87, doi: [10.1088/0004-637X/786/2/87](https://doi.org/10.1088/0004-637X/786/2/87)

Brooks, A. M., Solomon, A. R., Governato, F., et al. 2011, *ApJ*, 728, 51, doi: [10.1088/0004-637X/728/1/51](https://doi.org/10.1088/0004-637X/728/1/51)

Brown, T. M., Tumlinson, J., Geha, M., et al. 2012, *ApJL*, 753, L21, doi: [10.1088/2041-8205/753/1/L21](https://doi.org/10.1088/2041-8205/753/1/L21)

—. 2014, *ApJ*, 796, 91, doi: [10.1088/0004-637X/796/2/91](https://doi.org/10.1088/0004-637X/796/2/91)

Bullock, J. S., Kravtsov, A. V., & Weinberg, D. H. 2000, *ApJ*, 539, 517, doi: [10.1086/309279](https://doi.org/10.1086/309279)

Carlin, J. L., Sand, D. J., Price, P., et al. 2016, *ApJL*, 828, L5, doi: [10.3847/2041-8205/828/1/L5](https://doi.org/10.3847/2041-8205/828/1/L5)

Christensen, C., Quinn, T., Governato, F., et al. 2012, *MNRAS*, 425, 3058, doi: [10.1111/j.1365-2966.2012.21628.x](https://doi.org/10.1111/j.1365-2966.2012.21628.x)

Christensen, C. R., Brooks, A. M., Fisher, D. B., et al. 2014a, *MNRAS*, 440, L51, doi: [10.1093/mnrasl/slu020](https://doi.org/10.1093/mnrasl/slu020)

Christensen, C. R., Davé, R., Governato, F., et al. 2016, *ApJ*, 824, 57, doi: [10.3847/0004-637X/824/1/57](https://doi.org/10.3847/0004-637X/824/1/57)

Christensen, C. R., Governato, F., Quinn, T., et al. 2014b, *MNRAS*, 440, 2843, doi: [10.1093/mnras/stu399](https://doi.org/10.1093/mnras/stu399)

Clark, P. C., & Glover, S. C. O. 2014, *MNRAS*, 444, 2396, doi: [10.1093/mnras/stu1589](https://doi.org/10.1093/mnras/stu1589)

Corlies, L., Johnston, K. V., & Wise, J. H. 2018, *MNRAS*, 475, 4868, doi: [10.1093/mnras/sty064](https://doi.org/10.1093/mnras/sty064)

Danieli, S., van Dokkum, P., & Conroy, C. 2018, *ApJ*, 856, 69, doi: [10.3847/1538-4357/aaadfb](https://doi.org/10.3847/1538-4357/aaadfb)

Deason, A. J., Wetzel, A. R., Garrison-Kimmel, S., & Belokurov, V. 2015, *MNRAS*, 453, 3568, doi: [10.1093/mnras/stv1939](https://doi.org/10.1093/mnras/stv1939)

Diemand, J., Madau, P., & Moore, B. 2005, *MNRAS*, 364, 367, doi: [10.1111/j.1365-2966.2005.09604.x](https://doi.org/10.1111/j.1365-2966.2005.09604.x)

Dijkstra, M., Haiman, Z., Rees, M. J., & Weinberg, D. H. 2004, *ApJ*, 601, 666, doi: [10.1086/380603](https://doi.org/10.1086/380603)

Dobbs, C. L., Burkert, A., & Pringle, J. E. 2011, *MNRAS*, 417, 1318, doi: [10.1111/j.1365-2966.2011.19346.x](https://doi.org/10.1111/j.1365-2966.2011.19346.x)

D’Onghia, E., & Lake, G. 2008, *ApJL*, 686, L61, doi: [10.1086/592995](https://doi.org/10.1086/592995)

Dooley, G. A., Peter, A. H. G., Carlin, J. L., et al. 2017a, MNRAS, 472, 1060, doi: [10.1093/mnras/stx2001](https://doi.org/10.1093/mnras/stx2001)

Dooley, G. A., Peter, A. H. G., Yang, T., et al. 2017b, MNRAS, 471, 4894, doi: [10.1093/mnras/stx1900](https://doi.org/10.1093/mnras/stx1900)

Drlica-Wagner, A., Bechtol, K., Rykoff, E. S., et al. 2015, ApJ, 813, 109, doi: [10.1088/0004-637X/813/2/109](https://doi.org/10.1088/0004-637X/813/2/109)

Drlica-Wagner, A., Bechtol, K., Allam, S., et al. 2016, ApJL, 833, L5, doi: [10.3847/2041-8205/833/1/L5](https://doi.org/10.3847/2041-8205/833/1/L5)

Efstathiou, G. 1992, MNRAS, 256, 43P, doi: [10.1093/mnras/256.1.43P](https://doi.org/10.1093/mnras/256.1.43P)

Errani, R., Peñarrubia, J., & Walker, M. G. 2018, ArXiv e-prints. <https://arxiv.org/abs/1805.00484>

Farber, R., Ruszkowski, M., Yang, H.-Y. K., & Zweibel, E. G. 2018, ApJ, 856, 112, doi: [10.3847/1538-4357/aab26d](https://doi.org/10.3847/1538-4357/aab26d)

Fattahi, A., Navarro, J. F., Sawala, T., et al. 2016, MNRAS, 457, 844, doi: [10.1093/mnras/stv2970](https://doi.org/10.1093/mnras/stv2970)

Faucher-Giguère, C.-A., Lidz, A., Zaldarriaga, M., & Hernquist, L. 2009, ApJ, 703, 1416, doi: [10.1088/0004-637X/703/2/1416](https://doi.org/10.1088/0004-637X/703/2/1416)

Faucher-Giguère, C.-A., Quataert, E., & Hopkins, P. F. 2013, MNRAS, 433, 1970, doi: [10.1093/mnras/stt866](https://doi.org/10.1093/mnras/stt866)

Fry, A. B., Governato, F., Pontzen, A., et al. 2015, MNRAS, 452, 1468, doi: [10.1093/mnras/stv1330](https://doi.org/10.1093/mnras/stv1330)

Garrison-Kimmel, S., Boylan-Kolchin, M., Bullock, J. S., & Lee, K. 2014, MNRAS, 438, 2578, doi: [10.1093/mnras/stt2377](https://doi.org/10.1093/mnras/stt2377)

Garrison-Kimmel, S., Bullock, J. S., Boylan-Kolchin, M., & Bardwell, E. 2017a, MNRAS, 464, 3108, doi: [10.1093/mnras/stw2564](https://doi.org/10.1093/mnras/stw2564)

Garrison-Kimmel, S., Wetzel, A., Bullock, J. S., et al. 2017b, MNRAS, 471, 1709, doi: [10.1093/mnras/stx1710](https://doi.org/10.1093/mnras/stx1710)

Gill, S. P. D., Knebe, A., & Gibson, B. K. 2004, MNRAS, 351, 399, doi: [10.1111/j.1365-2966.2004.07786.x](https://doi.org/10.1111/j.1365-2966.2004.07786.x)

Glover, S. C. O., & Clark, P. C. 2012, MNRAS, 421, 116, doi: [10.1111/j.1365-2966.2011.20260.x](https://doi.org/10.1111/j.1365-2966.2011.20260.x)

Gnedin, N. Y. 2000, ApJ, 535, 530

Gnedin, N. Y., & Kravtsov, A. V. 2010, ApJ, 714, 287, doi: [10.1088/0004-637X/714/1/287](https://doi.org/10.1088/0004-637X/714/1/287)

—. 2011, ApJ, 728, 88, doi: [10.1088/0004-637X/728/2/88](https://doi.org/10.1088/0004-637X/728/2/88)

Gnedin, N. Y., Tassis, K., & Kravtsov, A. V. 2009a, ApJ, 697, 55, doi: [10.1088/0004-637X/697/1/55](https://doi.org/10.1088/0004-637X/697/1/55)

—. 2009b, ApJ, 697, 55, doi: [10.1088/0004-637X/697/1/55](https://doi.org/10.1088/0004-637X/697/1/55)

Governato, F., Brook, C., Mayer, L., et al. 2010, Nature, 463, 203, doi: [10.1038/nature08640](https://doi.org/10.1038/nature08640)

Haardt, F., & Madau, P. 2012, ApJ, 746, 125, doi: [10.1088/0004-637X/746/2/125](https://doi.org/10.1088/0004-637X/746/2/125)

Haiman, Z., Rees, M. J., & Loeb, A. 1996, ApJ, 467, 522, doi: [10.1086/177628](https://doi.org/10.1086/177628)

—. 1997, ApJ, 476, 458, doi: [10.1086/303647](https://doi.org/10.1086/303647)

Hoeft, M., Yepes, G., Gottlöber, S., & Springel, V. 2006, MNRAS, 371, 401, doi: [10.1111/j.1365-2966.2006.10678.x](https://doi.org/10.1111/j.1365-2966.2006.10678.x)

Homma, D., Chiba, M., Okamoto, S., et al. 2018, PASJ, 70, S18, doi: [10.1093/pasj/psx050](https://doi.org/10.1093/pasj/psx050)

Hopkins, P. F., Kereš, D., Oñorbe, J., et al. 2014, MNRAS, 445, 581, doi: [10.1093/mnras/stu1738](https://doi.org/10.1093/mnras/stu1738)

Hopkins, P. F., Narayanan, D., & Murray, N. 2013, MNRAS, 432, 2647, doi: [10.1093/mnras/stt723](https://doi.org/10.1093/mnras/stt723)

Hopkins, P. F., Quataert, E., & Murray, N. 2011, MNRAS, 417, 950, doi: [10.1111/j.1365-2966.2011.19306.x](https://doi.org/10.1111/j.1365-2966.2011.19306.x)

—. 2012, MNRAS, 421, 3522, doi: [10.1111/j.1365-2966.2012.20593.x](https://doi.org/10.1111/j.1365-2966.2012.20593.x)

Hopkins, P. F., Wetzel, A., Kereš, D., et al. 2018, MNRAS, 480, 800, doi: [10.1093/mnras/sty1690](https://doi.org/10.1093/mnras/sty1690)

Jeon, M., Besla, G., & Bromm, V. 2017, ApJ, 848, 85, doi: [10.3847/1538-4357/aa8c80](https://doi.org/10.3847/1538-4357/aa8c80)

Jethwa, P., Erkal, D., & Belokurov, V. 2016, MNRAS, 461, 2212, doi: [10.1093/mnras/stw1343](https://doi.org/10.1093/mnras/stw1343)

—. 2018, MNRAS, 473, 2060, doi: [10.1093/mnras/stx2330](https://doi.org/10.1093/mnras/stx2330)

Kallivayalil, N., Sales, L., Zivick, P., et al. 2018, ArXiv e-prints. <https://arxiv.org/abs/1805.01448>

Katz, N., & White, S. D. M. 1993, ApJ, 412, 455

Kim, C.-G., Kim, W.-T., & Ostriker, E. C. 2011, ApJ, 743, 25, doi: [10.1088/0004-637X/743/1/25](https://doi.org/10.1088/0004-637X/743/1/25)

Kim, C.-G., Ostriker, E. C., & Kim, W.-T. 2013, ApJ, 776, 1, doi: [10.1088/0004-637X/776/1/1](https://doi.org/10.1088/0004-637X/776/1/1)

Kim, D., & Jerjen, H. 2015, ApJL, 808, L39, doi: [10.1088/2041-8205/808/2/L39](https://doi.org/10.1088/2041-8205/808/2/L39)

Kim, D., Jerjen, H., Mackey, D., Da Costa, G. S., & Milone, A. P. 2015, ApJL, 804, L44, doi: [10.1088/2041-8205/804/2/L44](https://doi.org/10.1088/2041-8205/804/2/L44)

Kim, J.-h., Abel, T., Agertz, O., et al. 2014, ApJS, 210, 14, doi: [10.1088/0067-0049/210/1/14](https://doi.org/10.1088/0067-0049/210/1/14)

Kim, J.-h., Agertz, O., Teyssier, R., et al. 2016, ApJ, 833, 202, doi: [10.3847/1538-4357/833/2/202](https://doi.org/10.3847/1538-4357/833/2/202)

Knollmann, S. R., & Knebe, A. 2009, ApJS, 182, 608, doi: [10.1088/0067-0049/182/2/608](https://doi.org/10.1088/0067-0049/182/2/608)

Koposov, S. E., Belokurov, V., Torrealba, G., & Evans, N. W. 2015, ApJ, 805, 130, doi: [10.1088/0004-637X/805/2/130](https://doi.org/10.1088/0004-637X/805/2/130)

Kravtsov, A. V., Gnedin, O. Y., & Klypin, A. A. 2004, ApJ, 609, 482

Krumholz, M. R. 2012, ApJ, 759, 9, doi: [10.1088/0004-637X/759/1/9](https://doi.org/10.1088/0004-637X/759/1/9)

Krumholz, M. R., & Gnedin, N. Y. 2011, ApJ, 729, 36, doi: [10.1088/0004-637X/729/1/36](https://doi.org/10.1088/0004-637X/729/1/36)

Krumholz, M. R., Leroy, A. K., & McKee, C. F. 2011, ApJ, 731, 25, doi: [10.1088/0004-637X/731/1/25](https://doi.org/10.1088/0004-637X/731/1/25)

Krumholz, M. R., McKee, C. F., & Tumlinson, J. 2008, ApJ, 689, 865, doi: [10.1086/592490](https://doi.org/10.1086/592490)

—. 2009, *ApJ*, 693, 216, doi: [10.1088/0004-637X/693/1/216](https://doi.org/10.1088/0004-637X/693/1/216)

Kuhlen, M., Krumholz, M. R., Madau, P., Smith, B. D., & Wise, J. 2012, *ApJ*, 749, 36, doi: [10.1088/0004-637X/749/1/36](https://doi.org/10.1088/0004-637X/749/1/36)

Kuhlen, M., Madau, P., & Krumholz, M. R. 2013, *ApJ*, 776, 34, doi: [10.1088/0004-637X/776/1/34](https://doi.org/10.1088/0004-637X/776/1/34)

Laevens, B. P. M., Martin, N. F., Bernard, E. J., et al. 2015, *ApJ*, 813, 44, doi: [10.1088/0004-637X/813/1/44](https://doi.org/10.1088/0004-637X/813/1/44)

Laporte, C. F. P., Gómez, F. A., Besla, G., Johnston, K. V., & Garavito-Camargo, N. 2018, *MNRAS*, 473, 1218, doi: [10.1093/mnras/stx2146](https://doi.org/10.1093/mnras/stx2146)

Li, T. S., Simon, J. D., Pace, A. B., et al. 2018, *ApJ*, 857, 145, doi: [10.3847/1538-4357/aab666](https://doi.org/10.3847/1538-4357/aab666)

Li, T. Y., Alvarez, M. A., Wechsler, R. H., & Abel, T. 2014, *ApJ*, 785, 134, doi: [10.1088/0004-637X/785/2/134](https://doi.org/10.1088/0004-637X/785/2/134)

Li, Y.-S., & Helmi, A. 2008, *MNRAS*, 385, 1365, doi: [10.1111/j.1365-2966.2008.12854.x](https://doi.org/10.1111/j.1365-2966.2008.12854.x)

Lin, W., & Ishak, M. 2016, *JCAP*, 10, 025, doi: [10.1088/1475-7516/2016/10/025](https://doi.org/10.1088/1475-7516/2016/10/025)

Luque, E., Pieres, A., Santiago, B., et al. 2017, *MNRAS*, 468, 97, doi: [10.1093/mnras/stx405](https://doi.org/10.1093/mnras/stx405)

Mac Low, M.-M., & Glover, S. C. O. 2012, *ApJ*, 746, 135, doi: [10.1088/0004-637X/746/2/135](https://doi.org/10.1088/0004-637X/746/2/135)

Madau, P., Kuhlen, M., Diemand, J., et al. 2008, *ApJL*, 689, L41, doi: [10.1086/595814](https://doi.org/10.1086/595814)

Martin, N. F., Nidever, D. L., Besla, G., et al. 2015, *ApJL*, 804, L5, doi: [10.1088/2041-8205/804/1/L5](https://doi.org/10.1088/2041-8205/804/1/L5)

McConnachie, A. W. 2012, *AJ*, 144, 4, doi: [10.1088/0004-6256/144/1/4](https://doi.org/10.1088/0004-6256/144/1/4)

Menon, H., Wesolowski, L., Zheng, G., et al. 2015, *Computational Astrophysics and Cosmology*, 2, 1, doi: [10.1186/s40668-015-0007-9](https://doi.org/10.1186/s40668-015-0007-9)

Munshi, F., Brooks, A. M., Applebaum, E., et al. 2017, *ArXiv e-prints*. <https://arxiv.org/abs/1705.06286>

Munshi, F., Governato, F., Brooks, A. M., et al. 2013, *ApJ*, 766, 56, doi: [10.1088/0004-637X/766/1/56](https://doi.org/10.1088/0004-637X/766/1/56)

Murray, N., Ménard, B., & Thompson, T. A. 2011, *ApJ*, 735, 66, doi: [10.1088/0004-637X/735/1/66](https://doi.org/10.1088/0004-637X/735/1/66)

Newton, O., Cautun, M., Jenkins, A., Frenk, C. S., & Helly, J. C. 2018, *MNRAS*, 479, 2853, doi: [10.1093/mnras/sty1085](https://doi.org/10.1093/mnras/sty1085)

Nichols, M., Colless, J., Colless, M., & Bland-Hawthorn, J. 2011, *ApJ*, 742, 110, doi: [10.1088/0004-637X/742/2/110](https://doi.org/10.1088/0004-637X/742/2/110)

Nickerson, S., Stinson, G., Couchman, H. M. P., Bailin, J., & Wadsley, J. 2011, *MNRAS*, 415, 257, doi: [10.1111/j.1365-2966.2011.18700.x](https://doi.org/10.1111/j.1365-2966.2011.18700.x)

Onorbe, J., Boylan-Kolchin, M., Bullock, J. S., et al. 2015, *MNRAS*, 454, 2092, doi: [10.1093/mnras/stv2072](https://doi.org/10.1093/mnras/stv2072)

Onorbe, J., Hennawi, J. F., & Lukić, Z. 2017, *ApJ*, 837, 106, doi: [10.3847/1538-4357/aa6031](https://doi.org/10.3847/1538-4357/aa6031)

Ocvirk, P., Gillet, N., Shapiro, P. R., et al. 2016, *MNRAS*, 463, 1462, doi: [10.1093/mnras/stw2036](https://doi.org/10.1093/mnras/stw2036)

Okamoto, T., & Frenk, C. S. 2009, *MNRAS*, 399, L174, doi: [10.1111/j.1745-3933.2009.00748.x](https://doi.org/10.1111/j.1745-3933.2009.00748.x)

Okamoto, T., Gao, L., & Theuns, T. 2008, *MNRAS*, 390, 920, doi: [10.1111/j.1365-2966.2008.13830.x](https://doi.org/10.1111/j.1365-2966.2008.13830.x)

O'Shea, B. W., Wise, J. H., Xu, H., & Norman, M. L. 2015, *ApJL*, 807, L12, doi: [10.1088/2041-8205/807/1/L12](https://doi.org/10.1088/2041-8205/807/1/L12)

Ostriker, E. C., McKee, C. F., & Leroy, A. K. 2010, *ApJ*, 721, 975, doi: [10.1088/0004-637X/721/2/975](https://doi.org/10.1088/0004-637X/721/2/975)

Pace, A. B., & Li, T. S. 2018, *ArXiv e-prints*. <https://arxiv.org/abs/1806.02345>

Pallottini, A., Ferrara, A., Bovino, S., et al. 2017, *MNRAS*, 471, 4128, doi: [10.1093/mnras/stx1792](https://doi.org/10.1093/mnras/stx1792)

Patel, E., Carlin, J. L., Tollerud, E. J., Collins, M. L. M., & Dooley, G. A. 2018, *MNRAS*, 480, 1883, doi: [10.1093/mnras/sty1946](https://doi.org/10.1093/mnras/sty1946)

Pawlak, A. H., Schaye, J., & Dalla Vecchia, C. 2015, *MNRAS*, 451, 1586, doi: [10.1093/mnras/stv976](https://doi.org/10.1093/mnras/stv976)

Peñarrubia, J., Benson, A. J., Walker, M. G., et al. 2010, *MNRAS*, 406, 1290, doi: [10.1111/j.1365-2966.2010.16762.x](https://doi.org/10.1111/j.1365-2966.2010.16762.x)

Peñarrubia, J., Gómez, F. A., Besla, G., Erkal, D., & Ma, Y.-Z. 2016, *MNRAS*, 456, L54, doi: [10.1093/mnrasl/slv160](https://doi.org/10.1093/mnrasl/slv160)

Pontzen, A., Governato, F., Pettini, M., et al. 2008, *MNRAS*, 390, 1349, doi: [10.1111/j.1365-2966.2008.13782.x](https://doi.org/10.1111/j.1365-2966.2008.13782.x)

Rashkov, V., Madau, P., Kuhlen, M., & Diemand, J. 2012, *ApJ*, 745, 142, doi: [10.1088/0004-637X/745/2/142](https://doi.org/10.1088/0004-637X/745/2/142)

Read, J. I., Agertz, O., & Collins, M. L. M. 2016, *MNRAS*, 459, 2573, doi: [10.1093/mnras/stw713](https://doi.org/10.1093/mnras/stw713)

Read, J. I., Iorio, G., Agertz, O., & Fraternali, F. 2017, *MNRAS*, 467, 2019, doi: [10.1093/mnras/stx147](https://doi.org/10.1093/mnras/stx147)

Robertson, B. E., & Kravtsov, A. V. 2008, *ApJ*, 680, 1083, doi: [10.1086/587796](https://doi.org/10.1086/587796)

Saitoh, T. R., Daisaka, H., Kokubo, E., et al. 2008, *PASJ*, 60, 667. <https://arxiv.org/abs/0802.0961>

Salem, M., Bryan, G. L., & Corlies, L. 2016, *MNRAS*, 456, 582, doi: [10.1093/mnras/stv2641](https://doi.org/10.1093/mnras/stv2641)

Sales, L. V., Navarro, J. F., Cooper, A. P., et al. 2011, *MNRAS*, 418, 648, doi: [10.1111/j.1365-2966.2011.19514.x](https://doi.org/10.1111/j.1365-2966.2011.19514.x)

Sales, L. V., Navarro, J. F., Kallivayalil, N., & Frenk, C. S. 2017, *MNRAS*, 465, 1879, doi: [10.1093/mnras/stw2816](https://doi.org/10.1093/mnras/stw2816)

Sales, L. V., Wang, W., White, S. D. M., & Navarro, J. F. 2013, *MNRAS*, 428, 573, doi: [10.1093/mnras/sts054](https://doi.org/10.1093/mnras/sts054)

Sawala, T., Frenk, C. S., Crain, R. A., et al. 2013, *MNRAS*, 431, 1366, doi: [10.1093/mnras/stt259](https://doi.org/10.1093/mnras/stt259)

Sawala, T., Scannapieco, C., & White, S. 2012, *MNRAS*, 420, 1714, doi: [10.1111/j.1365-2966.2011.20181.x](https://doi.org/10.1111/j.1365-2966.2011.20181.x)

Sawala, T., Frenk, C. S., Fattahi, A., et al. 2015, MNRAS, 448, 2941, doi: [10.1093/mnras/stu2753](https://doi.org/10.1093/mnras/stu2753)

—. 2016, MNRAS, 456, 85, doi: [10.1093/mnras/stv2597](https://doi.org/10.1093/mnras/stv2597)

Schewtschenko, J. A., & Macciò, A. V. 2011, MNRAS, 413, 878, doi: [10.1111/j.1365-2966.2010.18179.x](https://doi.org/10.1111/j.1365-2966.2010.18179.x)

Semenov, V. A., Kravtsov, A. V., & Gnedin, N. Y. 2016, ApJ, 826, 200, doi: [10.3847/0004-637X/826/2/200](https://doi.org/10.3847/0004-637X/826/2/200)

—. 2018, ApJ, 861, 4, doi: [10.3847/1538-4357/aac6eb](https://doi.org/10.3847/1538-4357/aac6eb)

Sharma, M., & Nath, B. B. 2012, ApJ, 750, 55, doi: [10.1088/0004-637X/750/1/55](https://doi.org/10.1088/0004-637X/750/1/55)

Shen, S., Madau, P., Conroy, C., Governato, F., & Mayer, L. 2014, ApJ, 792, 99, doi: [10.1088/0004-637X/792/2/99](https://doi.org/10.1088/0004-637X/792/2/99)

Shen, S., Wadsley, J., & Stinson, G. 2010, MNRAS, 407, 1581, doi: [10.1111/j.1365-2966.2010.17047.x](https://doi.org/10.1111/j.1365-2966.2010.17047.x)

Simon, J. D., & Geha, M. 2007, ApJ, 670, 313, doi: [10.1086/521816](https://doi.org/10.1086/521816)

Simpson, C. M., Pakmor, R., Marinacci, F., et al. 2016, ApJL, 827, L29, doi: [10.3847/2041-8205/827/2/L29](https://doi.org/10.3847/2041-8205/827/2/L29)

Somerville, R. S. 2002, ApJL, 572, L23, doi: [10.1086/341444](https://doi.org/10.1086/341444)

Sternberg, A., Le Petit, F., Roueff, E., & Le Bourlot, J. 2014, ApJ, 790, 10, doi: [10.1088/0004-637X/790/1/10](https://doi.org/10.1088/0004-637X/790/1/10)

Stinson, G., Seth, A., Katz, N., et al. 2006, MNRAS, 373, 1074, doi: [10.1111/j.1365-2966.2006.11097.x](https://doi.org/10.1111/j.1365-2966.2006.11097.x)

Stinson, G. S., Bailin, J., Couchman, H., et al. 2010, MNRAS, 408, 812, doi: [10.1111/j.1365-2966.2010.17187.x](https://doi.org/10.1111/j.1365-2966.2010.17187.x)

Thompson, T. A., Quataert, E., & Murray, N. 2005, ApJ, 630, 167, doi: [10.1086/431923](https://doi.org/10.1086/431923)

Tollerud, E. J., Bullock, J. S., Strigari, L. E., & Willman, B. 2008, ApJ, 688, 277, doi: [10.1086/592102](https://doi.org/10.1086/592102)

Tollerud, E. J., & Peek, J. E. G. 2018, ApJ, 857, 45, doi: [10.3847/1538-4357/aab3e4](https://doi.org/10.3847/1538-4357/aab3e4)

Torrealba, G., Koposov, S. E., Belokurov, V., et al. 2016, MNRAS, 463, 712, doi: [10.1093/mnras/stw2051](https://doi.org/10.1093/mnras/stw2051)

Tremmel, M., Karcher, M., Governato, F., et al. 2017, MNRAS, 470, 1121, doi: [10.1093/mnras/stx1160](https://doi.org/10.1093/mnras/stx1160)

Visbal, E., Bryan, G. L., & Haiman, Z. 2017, MNRAS, 469, 1456, doi: [10.1093/mnras/stx909](https://doi.org/10.1093/mnras/stx909)

Visbal, E., Haiman, Z., & Bryan, G. L. 2015, MNRAS, 453, 4456, doi: [10.1093/mnras/stv1941](https://doi.org/10.1093/mnras/stv1941)

Visbal, E., Haiman, Z., Terrazas, B., Bryan, G. L., & Barkana, R. 2014, MNRAS, 445, 107, doi: [10.1093/mnras/stu1710](https://doi.org/10.1093/mnras/stu1710)

Wadsley, J. W., Keller, B. W., & Quinn, T. R. 2017, MNRAS, 471, 2357, doi: [10.1093/mnras/stx1643](https://doi.org/10.1093/mnras/stx1643)

Walsh, S. M., Willman, B., & Jerjen, H. 2009, AJ, 137, 450, doi: [10.1088/0004-6256/137/1/450](https://doi.org/10.1088/0004-6256/137/1/450)

Wang, L., Dutton, A. A., Stinson, G. S., et al. 2015, MNRAS, 454, 83, doi: [10.1093/mnras/stv1937](https://doi.org/10.1093/mnras/stv1937)

Weisz, D. R., Dolphin, A. E., Skillman, E. D., et al. 2014a, ApJ, 789, 147, doi: [10.1088/0004-637X/789/2/147](https://doi.org/10.1088/0004-637X/789/2/147)

—. 2014b, ApJ, 789, 148, doi: [10.1088/0004-637X/789/2/148](https://doi.org/10.1088/0004-637X/789/2/148)

Wheeler, C., Oñorbe, J., Bullock, J. S., et al. 2015, MNRAS, 453, 1305, doi: [10.1093/mnras/stv1691](https://doi.org/10.1093/mnras/stv1691)

Wise, J. H., Abel, T., Turk, M. J., Norman, M. L., & Smith, B. D. 2012, MNRAS, 427, 311, doi: [10.1111/j.1365-2966.2012.21809.x](https://doi.org/10.1111/j.1365-2966.2012.21809.x)

Wright, A. C., Brooks, A. M., Weisz, D. R., & Christensen, C. R. 2018, ArXiv e-prints, <https://arxiv.org/abs/1802.03019>

Yozin, C., & Bekki, K. 2015, MNRAS, 453, 2302, doi: [10.1093/mnras/stv1828](https://doi.org/10.1093/mnras/stv1828)

Zolotov, A., Brooks, A. M., Willman, B., et al. 2012, ApJ, 761, 71, <https://arxiv.org/abs/1207.0007>